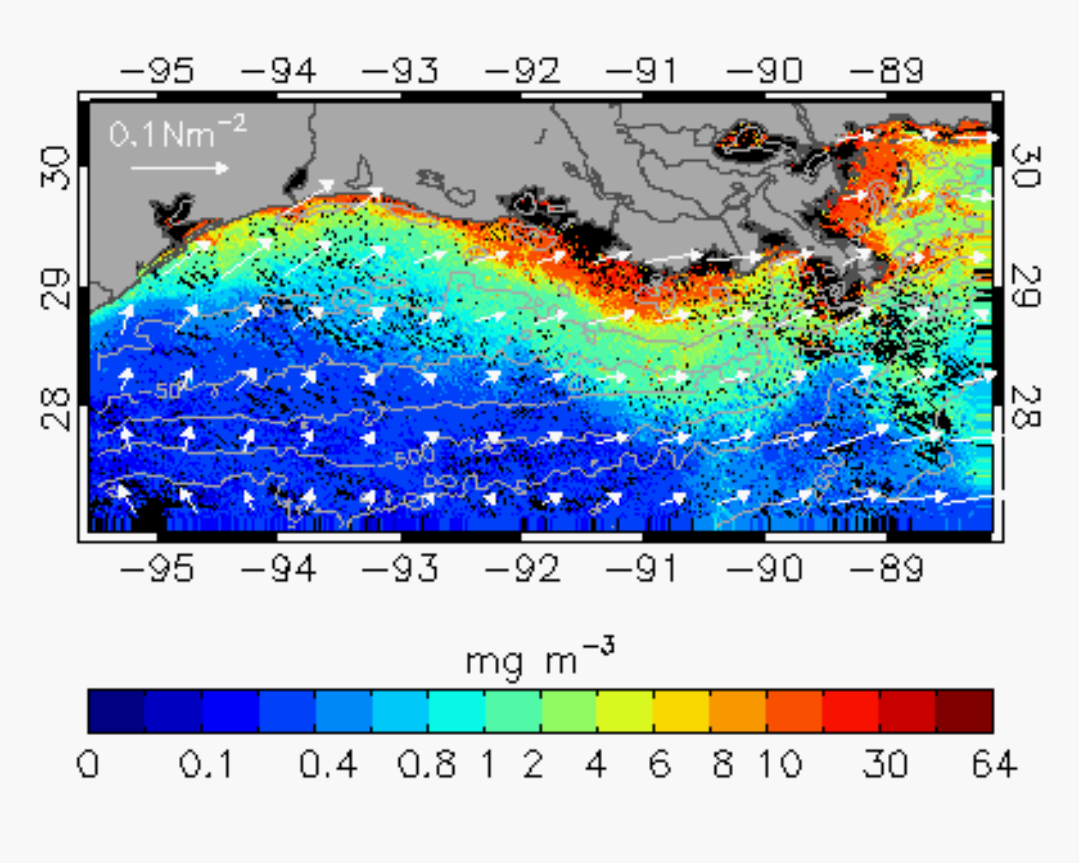
OCS Study
BOEM 2012-071

Coastal Marine Institute

Long-term Trends in Environmental Parameters along the Louisiana-Mississippi Outer Continental Shelf Using Remote-Sensing Data



BOEM Bureau of Ocean Energy Management

U.S. Department of the Interior
Bureau of Ocean Energy Management
Gulf of Mexico OCS Region

Cooperative Agreement
Coastal Marine Institute
Louisiana State University

OCS Study
BOEM 2012-071

Coastal Marine Institute

Long-term Trends in Environmental Parameters along the Louisiana-Mississippi Outer Continental Shelf Using Remote-Sensing Data

Author:

Eurico J. D'Sa

December 2012

Prepared under BOEM Cooperative Agreement
M08AX12685
by
Louisiana State University
Coastal Marine Institute
Baton Rouge, Louisiana 70803

Published by

U.S. Department of the Interior
Bureau of Ocean Energy Management
Gulf of Mexico OCS Region

Cooperative Agreement
Coastal Marine Institute
Louisiana State University

DISCLAIMER

This report was prepared under contract between the Bureau of Ocean Energy Management (BOEM) and Louisiana State University. This report has been technically reviewed by BOEM, and it has been approved for publication. Approval does not necessarily signify that the contents reflect the views and policies of BOEM, nor does mention of trade names or commercial products constitute endorsement or recommendation for use.

REPORT AVAILABILITY

To download a PDF file of this Gulf of Mexico OCS Region report, go to the U.S. Department of the Interior, Bureau of Ocean Energy Management, Environmental Studies Program Information System website and search on OCS Study BOEM 2012-071.

This report can be viewed at select Federal Depository Libraries. It can also be obtained from the National Technical Information Service; the contact information is below.

U.S. Department of Commerce
National Technical Information Service
5301 Shawnee Rd.
Springfield, Virginia 22312
Phone: (703) 605-6000, 1(800)553-6847
Fax: (703) 605-6900
Website: http://www.ntis.gov/

CITATION

D'Sa, E.J. **2012**. Long-term trends in environmental parameters along the Louisiana-Mississippi outer continental shelf using ocean color remote-sensing data. U.S. Dept. of the Interior, Bureau of Ocean Energy Management, Gulf of Mexico OCS Region, New Orleans, LA. OCS Study BOEM 2012-071. 35 pp.

ABOUT THE COVER

The cover image depicts SeaWiFS ocean color sensor-derived chlorophyll estimates during August 2008 along the Mississippi-Louisiana-Texas coast and the Outer Continental Shelf. QuikSCAT derived wind stress vectors (N m^{-2}) are superimposed on the SeaWiFS imagery.

ABSTRACT

The Mississippi River is the primary riverine source of freshwater, nutrients, organic/inorganic particulate and dissolved matter to the Louisiana continental shelf and strongly influences biogeochemical processes in the northern Gulf of Mexico (NGOM). The region is also an important center of economic activity associated with a well-developed fisheries and oil and gas industry. Ocean color remote sensing potentially provides the information on regional scales to address the issue of monitoring both short-term and long-term seawater particulate and dissolved matter distributions and an assessment of the effects of both anthropogenic and natural influences on coastal ecosystems. Sea-viewing Wide Field-of-view Sensor (SeaWiFS) satellite ocean color data together with field observations were used to examine the short-term, seasonal and long-term distribution of colored dissolved organic matter (CDOM) and chlorophyll along the coastal and shelf waters of the Mississippi, Louisiana, and part of Texas coast. A previously derived CDOM empirical algorithm was validated and used to derive estimates of surface CDOM absorption distribution at 412 nm from the SeaWiFS imagery. Spatial and temporal CDOM absorption distributions from satellite for the NGOM indicated strong seasonal influence associated with river discharge and effects of storms. Multiyear time-series satellite derived chlorophyll (Chl) estimates were used to examine the dominant scales of chlorophyll variability in the river-dominated coastal and oceanic waters. Wavelet analysis was applied to almost 10 years (1998-2007) of data and interpreted in conjunction with wind data from QuikSCAT satellite sensor to provide additional insights on the Chl variability in the region. Near the river deltas, seasonal maxima in peak variance were associated with seasonal peaks in river discharge, while in offshore waters similar peaks occurred with less regularity and appeared to be influenced mainly by the offshore wind stress that transported river plume waters with elevated Chl offshore. Although similar to the trends in the Mississippi River, Chl variability was lower in a zone off the Atchafalaya River while west of the Atchafalaya River, significant peaks in Chl variance appeared to be associated with the effects of Hurricane Rita in 2005.

CONTENTS

LIST OF FIGURES ix

ABBREVIATIONS AND ACRONYMS xi

1.0 INTRODUCTION 1

2.0 DATA AND METHODS 3
- **2.1 Study Area** 3
- **2.2 Field Bio-Optical Measurements** 3
- **2.3 Satellite Remote-Sensing Data Processing** 3
- **2.4 Time-Series Ocean Color Data Processing** 4

3.0 RESULTS 5
- **3.1 CDOM Optical Properties along the Louisiana Coast** 5
- **3.2 Seasonal and Storm Effects on CDOM in NGOM** 5
- **3.3 Long-Term Trends in Chlorophyll Distribution Using Wavelet Analysis** 6
  - **3.3.1 Chlorophyll Variability West of Mississippi River Delta (Zone 4)** 8
  - **3.3.2 Chlorophyll Variability off the Atchafalaya Delta (Zone 3)** 10
  - **3.3.3 Chlorophyll Variability West of the Atchafalaya River Delta (Zone 1)** 10

4.0 SUMMARY AND CONCLUSIONS 13

5.0 REFERENCES 15

APPENDIX A 19

LIST OF FIGURES

Figure 1. The study region in the northern Gulf of Mexico, showing the study domain extending from 27 to 30.5°N latitude, and 88.2 to 95.5°W longitude. Labels show the Mississippi River (MR), the Atchafalaya Rivers (AR), and southwest pass. 3

Figure 2. Seasonal surface CDOM absorption at 412 nm derived from SeaWiFS imagery for (a) winter (b) spring, (c) summer and (d) fall of 2005. 6

Figure 3. Study area in the northern Gulf of Mexico showing 5 zones and bathymetric contours at 20, 50, 100, 500, and 1000 m depth. AR and MR represent the locations of the Atchafalaya and Mississippi Rivers. The study region is divided into five zones: zone 4 is located immediately west of the Mississippi delta, zone 3 is off the Atchafalaya delta, and zone 1 is west of the Atchafalaya delta. 8

Figure 4. Mississippi River discharge measured at Tarbert Landing, Mississippi. Obtained from the U.S. Army Corps of Engineers Web site. 8

Figure 5. Figures a and b show wavelet power spectra (mg m^{-3})^2 of Chl averaged along the 20 and 500 m isobaths in Zone 4 immediately west of the Mississippi River delta. Figures c and d show corresponding scale-averaged time series for the period band 30-100 days; the green line shows the 95% confidence interval. 9

Figure 6. QuikSCAT satellite derived wind stress vectors (N m^{-2}) superimposed on SeaWiFS derived Chl (mg m^{-3}) for the months of (a) February 2004 and (b) March 2003. 9

Figure 7. Figures a and b show local wavelet power spectra (mg m^{-3})^2 of the time series Chl at 20 and 500 m isobaths in Zone 3 off the Atchafalaya River delta. Figures c and d show corresponding scale-averaged time series for the period band 30-100 days; the green line shows the 95% confidence interval. 10

Figure 8. (a) Local wavelet power spectra (mg m^{-3})^2 of the time series chlorophyll at 100 m isobath in zone 1 west of the Atchafalaya River delta. (b) Corresponding scale-averaged time series for the period band 30-100 days; the green line shows the 95% confidence interval. 11

Figure 9. QuikSCAT satellite derived wind stress vectors (N m^{-2}) superimposed on SeaWiFS derived chlorophyll (mg m^{-3}) for the month of September 2005. 12

ABBREVIATIONS AND ACRONYMS

CDOM	Colored Dissolved Organic Matter
Chl	chlorophyll concentration (mg m^{-3})
DAAC	NASA Goddard Distributed Active Archive Center
JPL	Jet Propulsion Laboratory
LA	Louisiana
LSU	Louisiana State University
MS	Mississippi
NASA	National Aeronautics and Space Administration
nm	nanometer
NGOM	Northern Gulf of Mexico
OCS	Outer Continental Shelf
SeaWiFS	Seawing Wide Field of View Sensor
SPM	Suspended Particulate Matter (mg L^{-1})

1.0 INTRODUCTION

The Mississippi River is the primary riverine source of freshwater, nutrients, organic and inorganic particulate, and dissolved matter to the Louisiana-Mississippi continental shelf and to the Gulf of Mexico (Lohrenz et al. 1997; 1999; 2008). The river-influenced coastal and offshore region is also of great ecological and economic importance to the region and the country. However, these regions are under the combined threats of subsidence, wetland loss, energetic meteorological events, and human-induced changes to the ecosystem (Rabalais et al. 2002). Many of these coastal regions are undergoing further population pressures, development and resource exploitation, while, at the same time, threats due to natural (storms, hurricanes, algal blooms) and anthropogenic hazards (oil spills, pollutant transport) are increasing. Information related to water masses and water quality indicators are important to support strategies for response, recovery, mitigation, and coastal restoration. Following Hurricanes Katrina and Rita, for example, there was a clear need to monitor water quality and transport of pollutants (e.g., oil spills) along the near-shore Gulf waters. Ocean color remote sensing potentially provides the information on regional scales to address the issue of monitoring both short-term and long-term seawater particulate and dissolved matter distributions and to assess the effects of both anthropogenic and natural influences on coastal ecosystems.

Satellite remote sensing makes it possible to conduct surveillance on large areas of the world's oceans for natural conditions and changes related to human activities. Plankton biomass, chlorophyll concentrations, colored dissolved organic material (CDOM), and other ocean color products are used in various ways to describe the water quality conditions and their positive or negative trends. In river-dominated areas, such as coastal Louisiana, the use of satellite imagery to monitor changes in water quality parameters is complicated by the variations due to characteristics of the river inflow and its contents (D'Sa et al. 2006; Walker and Rabalais 2006; D'Sa 2008; Green et al. 2008).

In this project, satellite ocean color data products, such as chlorophyll concentration and CDOM, were examined using a standard NASA and a regionally-developed CDOM absorption algorithm to improve our understanding and use of ocean color data for short- and long-term trends in their variability in the northern Gulf of Mexico (NGOM). A regional suspended particulate matter (SPM) algorithm (D'Sa et al. 2007) was also applied to SeaWiFS imagery to examine short-term (e.g., storms and hurricanes) (D'Sa and Ko 2008; D'Sa et al. 2011a) and long-term (D'Sa et al. 2011b) influences of river discharge and storms on SPM distribution in the NGOM.

With an annual discharge rate of approximately 19,000 m^3 s^{-1}, approximately 70% of the Mississippi River discharges into the Gulf of Mexico through the birdfoot delta and into deeper shelf waters, and the remaining 30% of the discharge is delivered by the Atchafalaya River into the broad Atchafalaya shelf, creating a major region of freshwater influence along the Louisiana, Mississippi, and Texas coast (Dinnel and Wiseman 1986). In coastal waters dissolved organic matter contribution to seawater comes from rivers and other terrestrial inputs. A significant proportion of dissolved organic matter in these waters is present as CDOM that influences ocean color, water quality, and remotely sensed signals (Carder et al. 1989). CDOM thus represents a fraction that can be determined through measurements of optical absorption of

filtered seawater and also through remote sensing. Light absorption by CDOM in the ultraviolet (UV) and visible wavelength range exhibits an exponential decay with increasing wavelength. Absorption of sunlight by CDOM can reduce light availability for primary production and also reduce the damaging effects of solar radiation in the ultraviolet. In the process CDOM can undergo photo-oxidation or photo-bleaching (Vodacek et al. 1997; D'Sa 2008; D'Sa and DiMarco 2009).

Because CDOM is an important component of dissolved organic matter in large river dominated margins, both field and ocean color remote sensing studies have been conducted in the coastal waters influenced by the Mississippi River system (Chen et al. 2004; Conmy et al. 2004; D'Sa et al. 2006; Del Castillo and Miller 2008; D'Sa 2008; D'Sa and DiMarco 2009). Studies of CDOM optical properties in the NGOM have indicated a highly variable distribution influenced mainly by the seasonal discharge from the Mississippi River (Chen et al. 2004; D'Sa and DiMarco 2009). However, other factors, such as in situ CDOM production associated with phytoplankton primary production or its bacterial decomposition and CDOM photo-bleaching, have also been found to influence CDOM variability in the study region (Chen et al. 2004; D'Sa and DiMarco 2009). Empirical ocean color remote sensing algorithms have been developed for various coastal regions, including the NGOM, for the determination of CDOM using remote sensing reflectance ratios and coefficients that have been regionally optimized (D'Sa and Miller 2003; D'Sa et al. 2006; Mannino et al. 2008). In this study we have examined CDOM and particulate optical properties along the Louisiana coast (D'Sa 2008; D'Sa and DiMarco 2009; Naik et al. in press) and further used a regional CDOM algorithm for SeaWiFS satellite sensor to examine the short-term and seasonal variability of CDOM absorption in coastal and oceanic waters extending from the Mississippi delta to Galveston, Texas. A seasonal increase in hurricane activity (e.g., Hurricane Rita) in the Gulf of Mexico in 2005 allowed for the assessment of hurricane and storm activity on CDOM distribution in the NGOM.

Another important water quality parameter in the NGOM is chlorophyll biomass, an indicator of productivity in the Gulf (Lohrenz et al. 1997; 1999). In addition to river discharge, chlorophyll concentrations are also influenced by cold fronts, wind-induced currents, and hurricanes that often impact the region (Walker et al. 2005; Walker and Rabalais 2006; D'Sa et al. 2006). Satellite ocean color chlorophyll estimates have provided a synoptic pattern of distribution along the Louisiana coast (D'Sa et al. 2006). The SeaWiFS satellite sensor has provided the longest record of ocean color data that has been used to examine trends in optical properties and phytoplankton chlorophyll distributions (Lohrenz et al. 2008; Greene and Gould 2008). In this study we use a 10-year record of SeaWiFS chlorophyll estimates in the NGOM to examine chlorophyll variability occurring at different temporal scales at different locations in the study area. We use wavelet analysis on time series data (D'Sa and Korobkin 2008a) to study the temporal variance in SeaWiFS derived chlorophyll by examining the dominant frequencies and their interannual variability in different regions of the NGOM.

2.0 DATA AND METHODS

2.1 STUDY AREA

The study area located in the Gulf of Mexico extends from 27-30.5° N latitude, 88.2-95.5° W longitude and includes coastal and OCS waters of the states of Mississippi, Louisiana, and part of Texas (Figure 1). Seasonal discharge from the Mississippi and Atchafalaya Rivers through the birdsfoot and Atchafalaya deltas results in a major region of freshwater influence along the coasts of Mississippi, Louisiana, and Texas. Additional outflows from the bays and smaller rivers can also contribute biogenic material and sediments to the shelf waters.

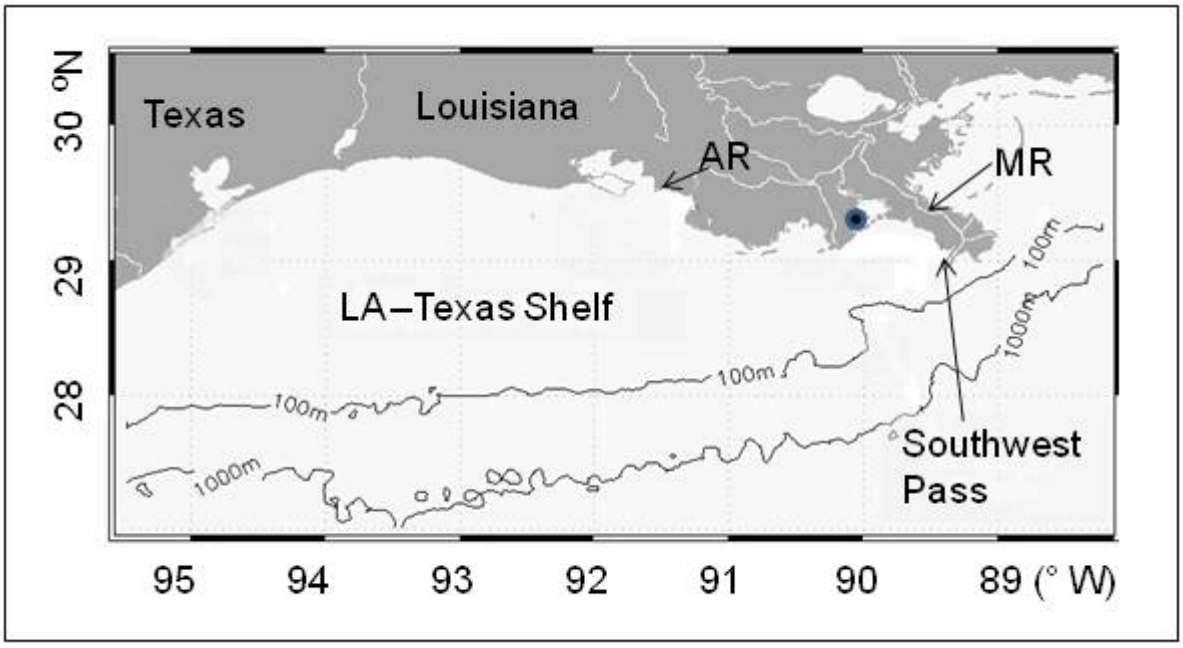


Figure 1. The study region in the northern Gulf of Mexico, showing the study domain extending from 27 to 30.5°N latitude, and 88.2 to 95.5°W longitude. Labels show the Mississippi River (MR), the Atchafalaya Rivers (AR), and Southwest Pass (SW Pass).

2.2 FIELD BIO-OPTICAL MEASUREMENTS

Field data processed and analyzed as part of this study were obtained during cruises in 2005, 2007, 2008, and 2009, along the Louisiana coast. They include field absorption measurements of CDOM and other constituents, such as phytoplankton and non-algal particles and are described in detail in D'Sa and DiMarco (2009) and Naik et al. (2011).

2.3 SATELLITE REMOTE-SENSING DATA PROCESSING

Satellite remote sensing data used in this study include mainly ocean color data from SeaWiFS satellite sensor. SeaWiFS Level L1A data was downloaded from NASA DAAC and processed using NASA's SeaDAS 5.1 processing software using a regional CDOM and SPM

algorithm (D'Sa et al. 2006 and 2007). SeaWiFS estimates of chlorophyll concentrations were obtained using the standard OC4 algorithm (O'Reilly et al. 1998). In addition, winds from QuikSCAT satellite sensor were downloaded from NASA JPL DAAC and processed using methods described in Sharma and D'Sa 2008.

2.4 TIME-SERIES OCEAN COLOR DATA PROCESSING

Level 1A SeaWiFS data for the NGOM from 1998 to 2007 were downloaded from NASA DAAC and processed to Level 2 Chl product at 2-km resolution for the study region. NASA default coefficients and the standard atmospheric correction algorithm and the standard OC4 algorithm were used to generate the Level 2 Chl, which were then composited into 15-day, monthly, or seasonal means to generate the time series data used in this study. Wavelet transform was applied to 15-day composite image data along bathymetric contour lines to examine long-term trends in their variability.

3.0 RESULTS

3.1 CDOM Optical Properties along the Louisiana Coast

Absorption properties of particulate and dissolved constituents of water along the Louisiana coast have been studied from data acquired during various field campaigns conducted both before and during the project (D'Sa and DiMarco 2009; Singh et al. 2010a, b; Naik et al. in press). Some details on CDOM absorption properties along the Louisiana coast are shown in Appendix A (D'Sa and DiMarco 2009); those of phytoplankton and non-algal absorption properties have been described in Naik et al. (in press). Briefly, a conservative relationship was observed between CDOM and salinity; also, seasonal changes in CDOM concentrations were observed that were attributed to sources (algal biomass) and sinks (photo-bleaching) of CDOM (D'Sa and DiMarco 2009).

3.2 Seasonal and Storm Effects on CDOM in NGOM

Short-term and seasonal estimates of CDOM absorption at 412 nm and surface salinity were derived from the SeaWiFS satellite data for the Louisiana-Texas coast during 2005 using an empirical CDOM algorithm and a conservative CDOM-salinity relationship (D'Sa et al. 2006; D'Sa and Korobkin 2008b; D'Sa and DiMarco 2009). Field measurements obtained during various seasons in 2005 indicated high correlations between field and satellite estimates of CDOM, suggesting satellite estimates to be a good representation of the surface CDOM and salinity fields. Discharge from the Mississippi and Atchafalaya Rivers strongly influenced the seasonal surface CDOM distribution. During fall and winter, frontal passages also influenced CDOM distribution over the shelf waters. Clear satellite imagery obtained before and after the passage of a cold front in March 2005 indicated a general decrease in surface CDOM and an offshore increase of elevated CDOM suggesting that frequent frontal passages contribute to mixing of riverine CDOM and its offshore transport (D'Sa and Korobkin 2008b). An examination of the spatial and temporal CDOM absorption distributions from SeaWiFS satellite data indicated strong seasonal influence associated with discharge from the Mississippi-Atchafalaya River system (Figure 2). A seasonal increase in storms and hurricanes allowed an assessment of the effects of Hurricane Rita in September 2005 (D'Sa and Korobkin 2008b).

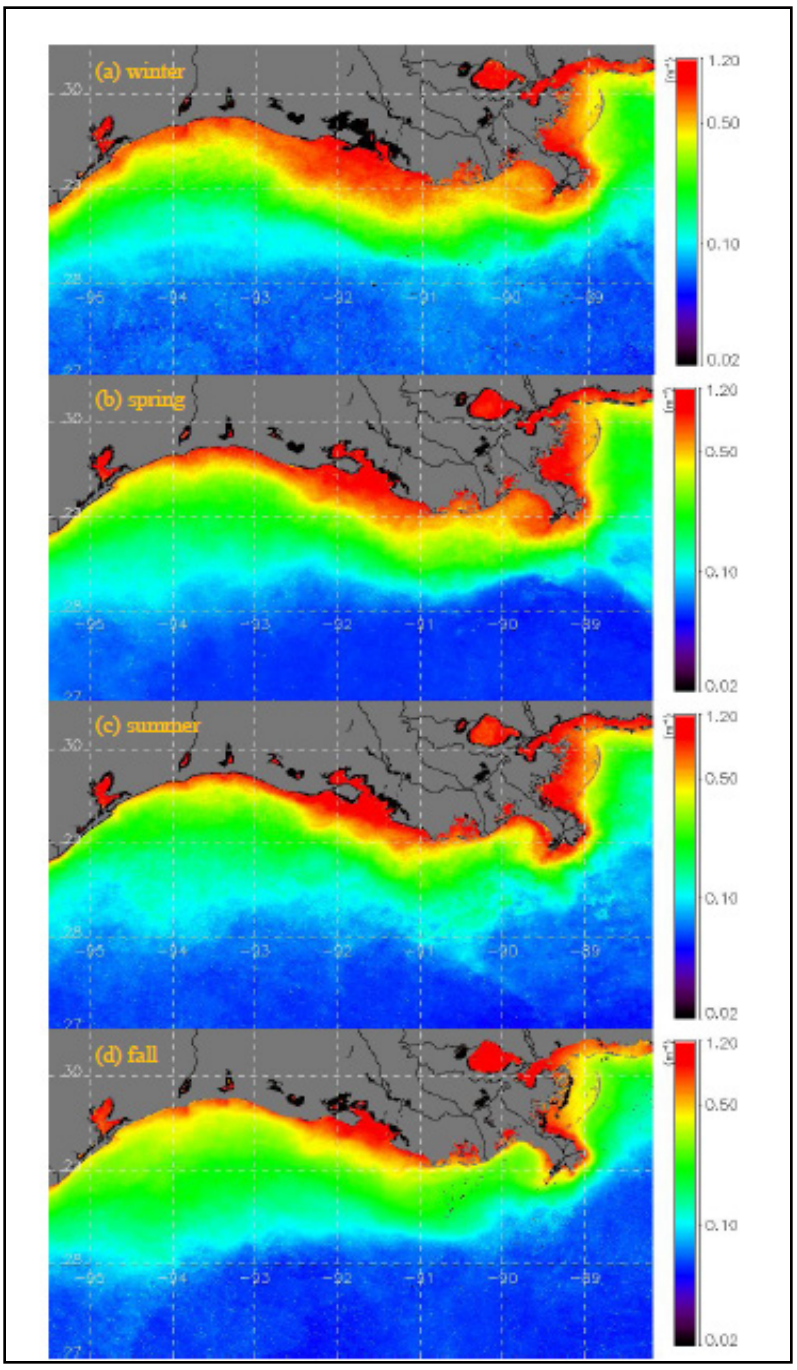


Figure 2. Seasonal surface CDOM absorption at 412 nm derived from SeaWiFS imagery for (a) winter (b) spring, (c) summer and (d) fall of 2005.

3.3 Long-Term Trends in Chlorophyll Distribution Using Wavelet Analysis

River discharge, cold fronts, wind induced currents, and hurricanes often influence the chlorophyll distribution in the NGOM (Walker et al. 2005; Walker and Rabalais 2006; D'Sa et

al. 2006; D'Sa and Korobkin 2009). Satellite ocean color Chl estimates have provided a synoptic pattern of distribution along the Louisiana coast (Walker and Rabalais 2006; Lohrenz et al. 2008). The SeaWiFS satellite sensor has provided the longest record of ocean color data that has been used to examine long-term trends in phytoplankton Chl distributions (Henson and Thomas 2007). In this study, we use a 10-year record of SeaWiFS Chl estimates in the NGOM to examine Chl variability occurring at different temporal scales at different locations in the study area. We use wavelet analysis on time series data (Morlet 1983; Machu et al. 1999; Henson and Thomas 2007) to study the temporal variance in SeaWiFS derived Chl by examining the dominant frequencies and their interannual variability along different bathymetric contours. To further examine the physical linkages we use QuikSCAT satellite derived monthly wind stress vectors superimposed on SeaWiFS Chl.

The study area shown in Figure 3 comprises the coastal states of Mississippi, Louisiana, and part of Texas extending between 88.2° - 95.5° W and into the Gulf of Mexico to 27.0° N latitude. Two main rivers discharging into the study area are the Mississippi and Atchafalaya Rivers. The Mississippi River discharge over a period from 1998 to 2008 is shown in Figure 2. Discharge from the Atchafalaya River (not shown) has the same seasonal variability but lower volume than the Mississippi River.

Level 1A SeaWiFS data for the NGOM between 1998 and 2007 were downloaded from NASA DAAC and processed to Level 2 Chl product at 2 km resolution for the study region. NASA default coefficients and the standard atmospheric correction algorithm and the standard OC4 algorithm were used to generate the Level 2 Chl which were then composited into 15-day means to generate the time series data used in this study. The study area was divided into five zones (Figure 3) and time series Chl anomalies were determined in zone 1, 3, and 4 along the 20, 100, and 500 m isobaths. Wavelet transform, a method that decomposes a signal into time-frequency space (Morlet 1983; Torrence and Compo 1998) was applied to the mean Chl anomaly data. The output of the wavelet transform is a local wavelet power spectrum (Figure 5a) that depicts the variance in Chl $((\text{mg m}^{-3})^2)$ and can be interpreted as a "map" of the time variability of dominant frequencies (Henson and Thomas 2007). Because the time series has finite length, errors increase at the edges of the wavelet spectrum and should be interpreted with caution (Torrence and Compo 1988). The normalized scale-averaged time series (Figure 5c) denotes the mean variance in the 30-100 period band and is obtained by normalizing the wavelet power by $N/2\sigma^2$ (where N is the number of data points and σ^2 is its variance); the green line denotes the 95% confidence level.

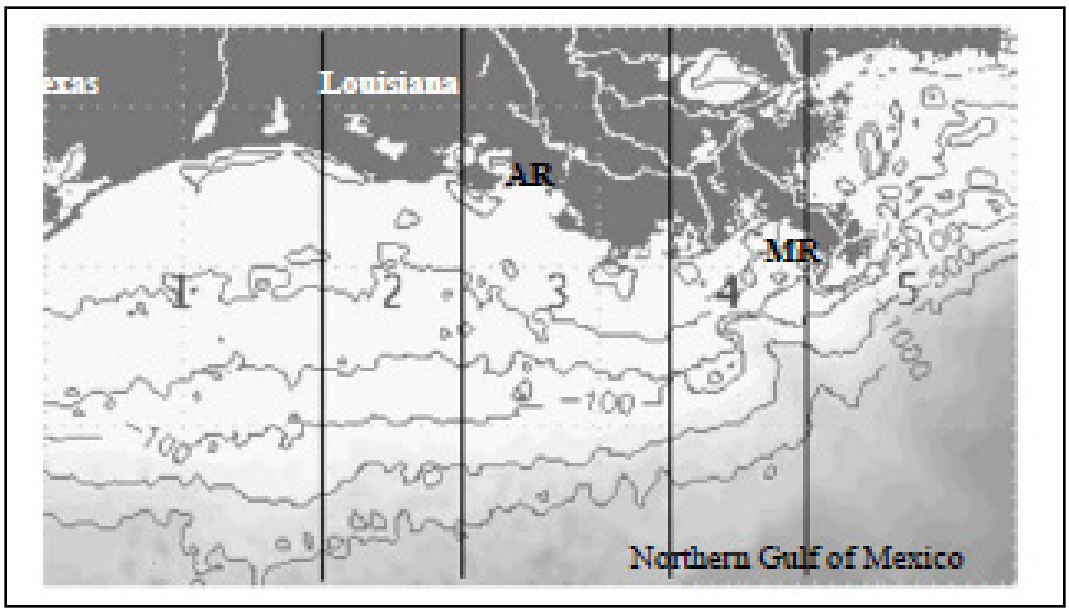


Figure 3. Study area in the northern Gulf of Mexico showing 5 zones and bathymetric contours at 20, 50, 100, 500, and 1000 m depth. AR and MR represent the locations of the Atchafalaya and Mississippi Rivers. The study region is divided into five zones: zone 4 is located immediately west of the Mississippi delta, zone 3 is off the Atchafalaya delta, and zone 1 is west of the Atchafalaya delta.

3.3.1 Chlorophyll Variability West of Mississippi River Delta (Zone 4)

Figure 4 shows the discharge from the Mississippi River for the period the time series SeaWiFS Chl data were analyzed using the wavelet transform (Figure 5). Seasonal variability with peaks in river discharge generally occurred in winter or spring, and a minimum in late summer. Highest discharge occurred in 1999, 2001, 2002, and 2005, and lowest discharge occurred in 2000 and 2006.

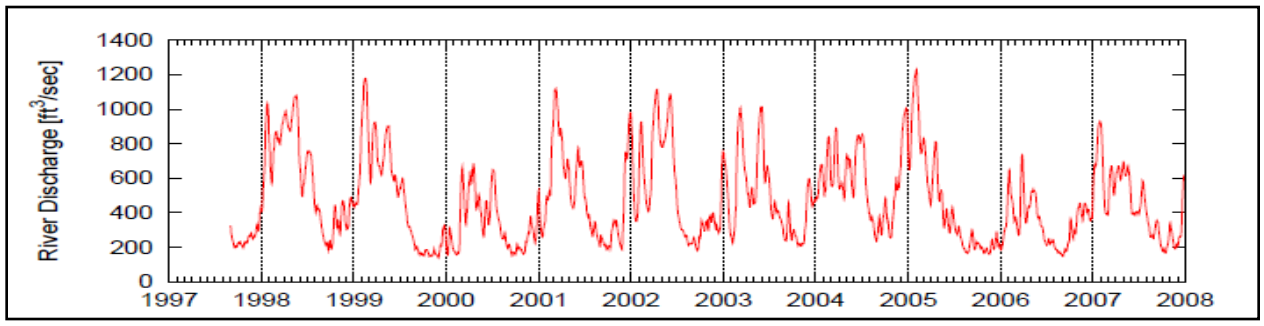


Figure 4. Mississippi River discharge measured at Tarbert Landing, Mississippi. Obtained from the U.S. Army Corps of Engineers Web site.

Figure 5a shows the time variability in the wavelet power peaks at the 20 m isobath in zone 4 (Figure 3), which occurs mainly in spring and occasionally in winter, that appears to coincide with peaks in river discharge. The dominant period of most of the peaks is approximately between 30 and 60 days. The strongest peak of wavelet power at the 20 m isobath occurred in

February 2004 that was related to a winter peak in river discharge and southerly wind stress over the region (Figure 6a). The normalized scale-averaged time series (averaged in the 30-100 day band) at the 20 m isobath (Figure 5c) further revealed the regular seasonal variability and the interannual differences in the wavelet power. At the 500 m isobath the wavelet power is weak most of the years; significant chlorophyll variability occurs in the spring of 1998, 2003, and 2007. As shown in Figure 6b, the increases in wavelet power during these events were related mainly to the peaks in river discharge and southerly wind stress. However, in comparison with the 20 m isobath, the dominant periods of some of the peaks in Chl variance were of longer duration at the 500 m isobath (Figure 5b).

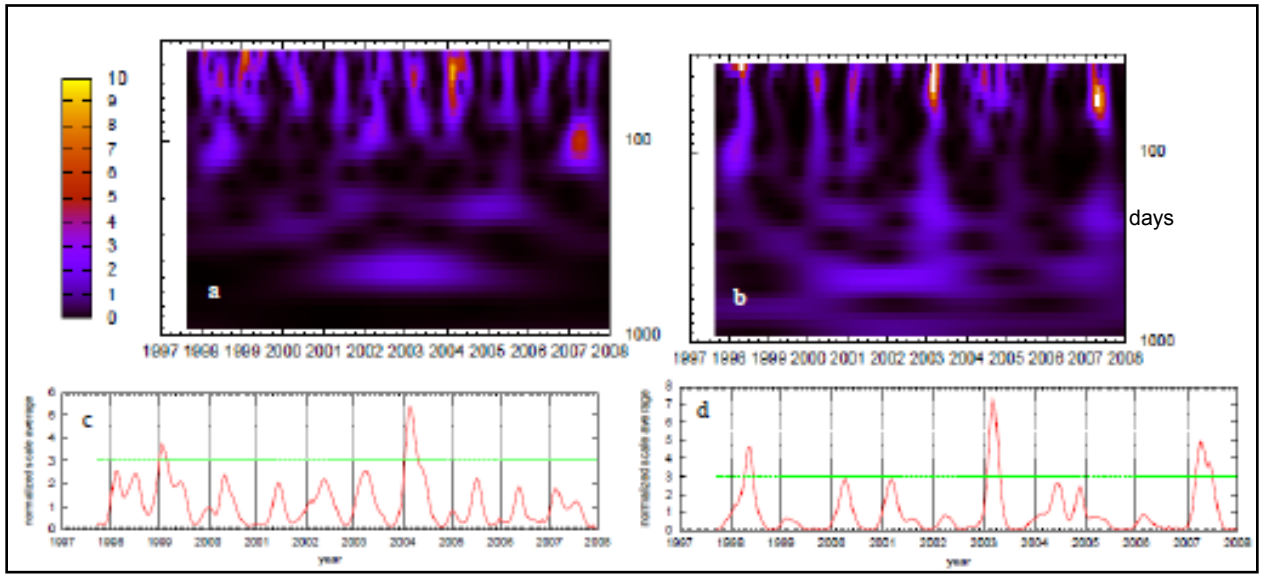


Figure 5. Figures a and b show wavelet power spectra (mg m-3)2 of Chl averaged along the 20 and 500 m isobaths in Zone 4 immediately west of the Mississippi River delta. Figures c and d show corresponding scale-averaged time series for the period band 30-100 days; the green line shows the 95% confidence interval.

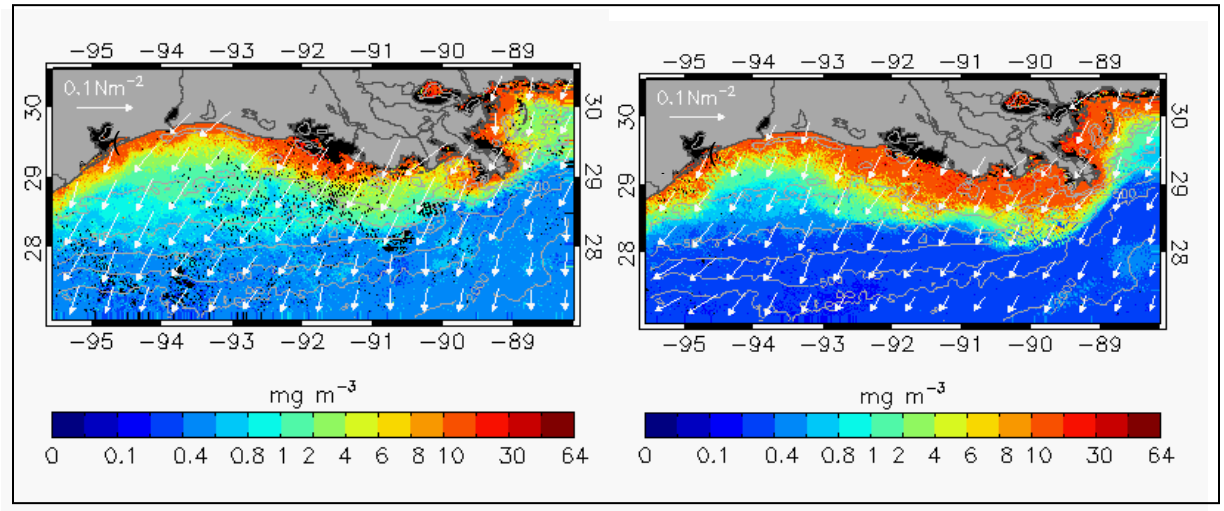


Figure 6. QuikSCAT satellite derived wind stress vectors (N m^{-2}) superimposed on SeaWiFS derived Chl (mg m^{-3}) for the months of (a) February 2004 and (b) March 2003.

3.3.2 Chlorophyll Variability off the Atchafalaya Delta (Zone 3)

At the 20 m isobath off the Atchafalaya River (Figure 3) seasonal peaks in wavelet power spectra were observed with interannual variability that appeared reduced during some years (Figures 7a, 7c) in comparison with those off the Mississippi River. The large peaks in January 1998 and February 2003 at the 20 m isobath were associated with northerly wind stress (not shown).

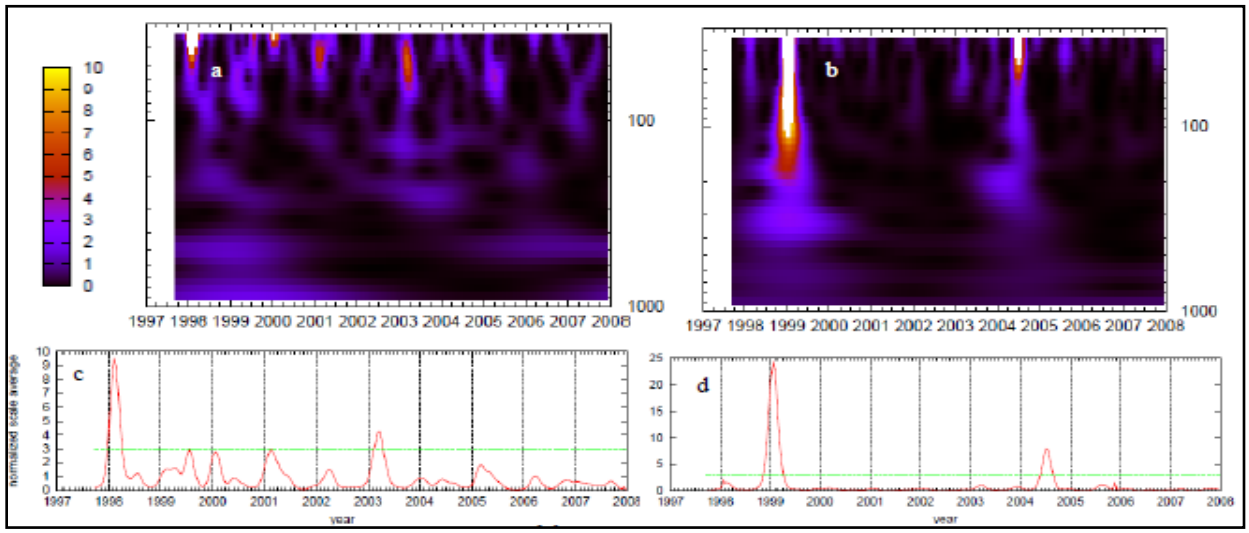


Figure 7. Figures a and b show local wavelet power spectra (mg m-3)2 of the time series Chl at 20 and 500 m isobaths in Zone 3 off the Atchafalaya River delta. Figures c and d show corresponding scale-averaged time series for the period band 30-100 days; the green line shows the 95% confidence interval.

A strong peak variance observed in January 1999 at the 500 m isobath (Figure 7b, d) appeared to be due to the offshore transport of a large Chl plume just east of the Atchafalaya Bay (not shown). The role of wind stress in driving these high Chl waters offshore could not be ascertained because QuikSCAT wind data was not available during this period.

3.3.3 Chlorophyll Variability West of the Atchafalaya River Delta (Zone 1)

A peak in wavelet power in June 2002 (Figure 8a and b) appeared to be linked to a peak in river discharge in early summer. West of the Atchafalaya River (zone 1) at the 100 m isobath, the strongest peak in wavelet power with a period of about 60 days appeared in September 2005 (Figure 8a and b). Hurricane Rita, which made landfall in zone 1, appeared to have a longer duration impact on the chlorophyll variability in the region; this is indicated in Figure 9, which shows the surface chlorophyll distribution for September 2005. A large patch of elevated chlorophyll observed in the region of zone 1 is unusual in this region and may have been due to nutrient discharged from the ponding of flooded waters due to the hurricane.

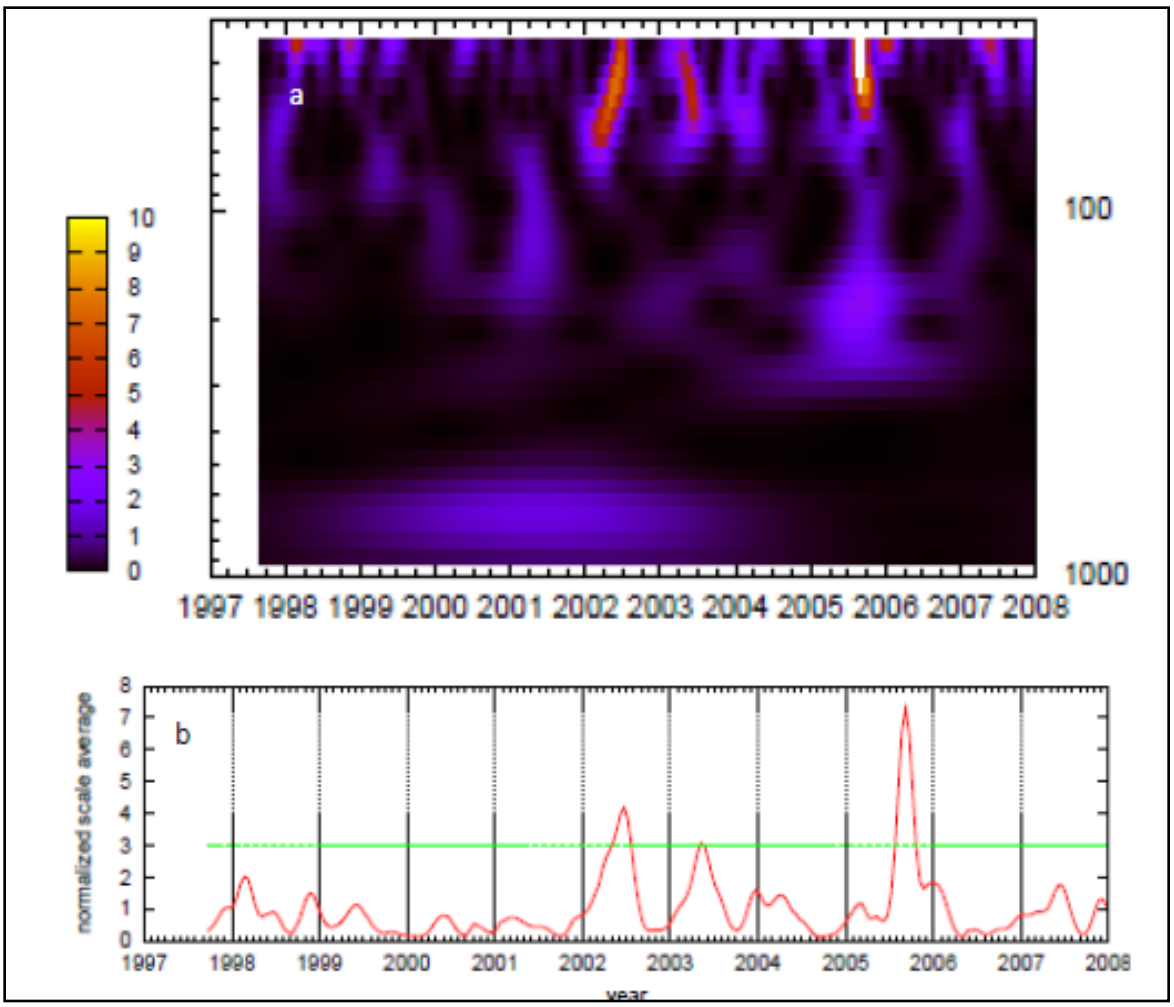


Figure 8. (a) Local wavelet power spectra (mg $m^{-3})^2$ of the time series chlorophyll at 100 m isobath in zone 1 west of the Atchafalaya River delta. (b) Corresponding scale-averaged time series for the period band 30-100 days; the green line shows the 95% confidence interval.

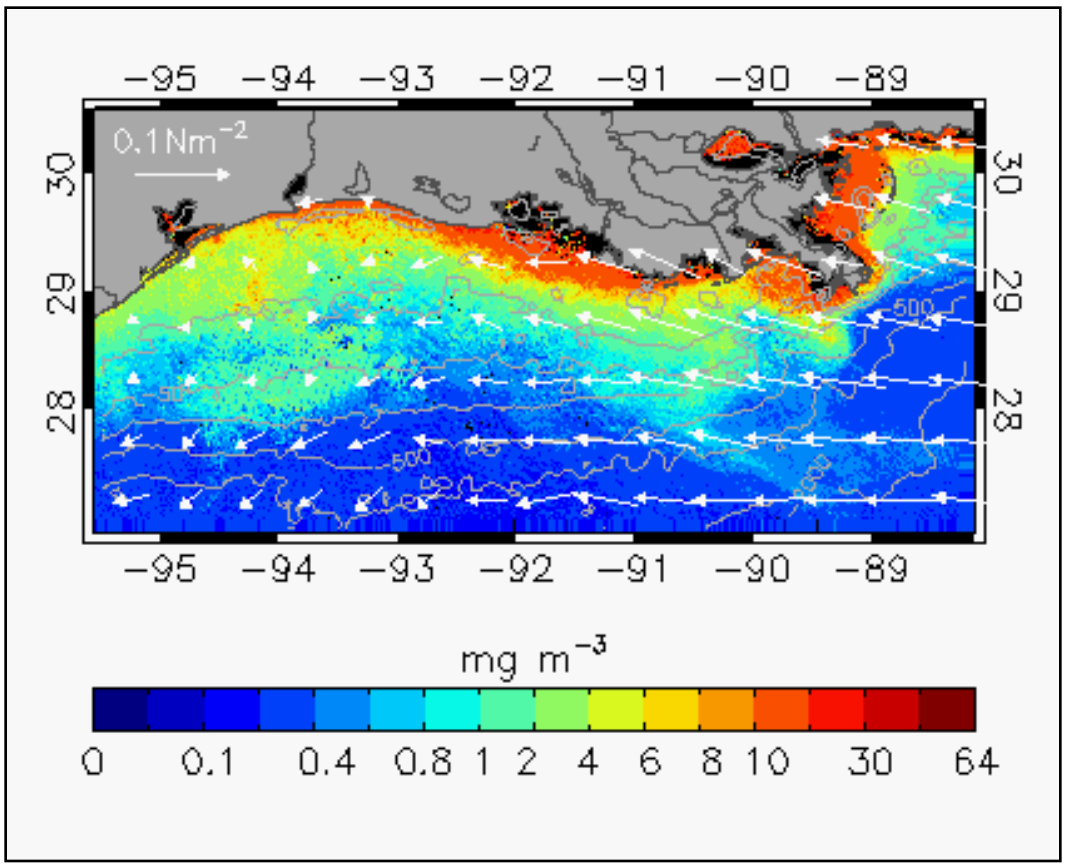


Figure 9. QuikSCAT satellite derived wind stress vectors (N m-2) superimposed on SeaWiFS derived chlorophyll (mg m-3) for the month of September 2005.

4.0 SUMMARY AND CONCLUSIONS

The Mississippi-Atchafalaya River system strongly influences the biogeochemical properties of the NGOM due to the discharge of freshwater and delivery of particulate and dissolved organic matter to the coastal waters. In this study we examined the spatial and temporal variation of CDOM absorption properties and chlorophyll concentrations along the Louisiana coast and the NGOM shelf waters. CDOM optical properties were found to be strongly influenced by riverine discharge. Additional factors, such as photobleaching and in situ biological production, also influenced the CDOM absorption properties. Estimates of seasonal distribution of CDOM obtained from SeaWiFS satellite data indicated highest levels of CDOM in the nearshore waters in winter; these gradually decreased in spring, summer, and fall, and are potentially associated with a contraction of the nearshore region of freshwater influence. The seasonal impact of storms and hurricanes on CDOM distribution were studied using SeaWiFS CDOM imagery obtained before and after Hurricane Rita made landfall near the Texas-Louisiana border. A comparison of the CDOM imagery indicated a decrease in CDOM and an increase in salinity of the nearshore waters, suggesting an intrusion of marine waters due to Hurricane Rita. The application of wavelet analysis to the time series SeaWiFS data revealed different scales of variability along the Louisiana coast, a region that is strongly influenced by the discharge from the Atchafalaya and Mississippi Rivers. The seasonal river discharge appears to strongly influence the timing of the peak variance in waters that are directly influenced by the two rivers. The use of monthly QuikSCAT derived wind stress vectors superimposed on monthly Chl maps provided some insights into the Chl variance determined by wavelet analysis. Away from the river influence the interannual peaks in Chl variance were weak with strongest wavelet power peak associated with hurricane activity in 2005.

5.0 REFERENCES

Carder, K.L., R.G. Steward, and G.R. Ortner. **1989**. Marine and fulvic acids: their effect on remote sensing of ocean chlorophyll. *Limnology and Oceanography* 34:68-81.

Chen, R.F., P. Bissett, P.G. Coble, R. Conmy, G.B. Gardner, M.A. Moran, X. Wang, M.L. Wells, P. Whelan, and R.G. Zepp. **2004**. Chromophoric dissolved organic matter (CDOM) source characterization in the Louisiana Bight. *Marine Chemistry* 89:257-272.

Conmy, R.N., P.G. Coble, R.F. Chen, and G.B. Gardner. **2004**. Optical properties of colored dissolved organic matter in the Northern Gulf of Mexico. *Marine Chemistry* 89:127-144.

Dinnel, S.P. and W.J. Wiseman. **1986**. Freshwater on the Louisiana and Texas Shelf. *Continental Shelf Research* 6:765–784.

Del Castillo, C.E. and R.L. Miller. **2008**. On the use of ocean color remote sensing to measure the transport of dissolved organic carbon by the Mississippi River Plume. *Remote Sensing of the Environment* 112:836-844.

D'Sa, E.J. **2008**. Colored dissolved organic matter in coastal waters influenced by the Atchafalaya River, USA: effects of an algal bloom. *Journal of Applied Remote Sensing 2:023502*.

D'Sa, E.J. and S.F. DiMarco. **2009**. Seasonal variability and controls on chromophoric dissolved organic matter in a large river-dominated coastal margin. *Limnology and Oceanography* 54:2233–2242.

D'Sa, E.J. and D.S. Ko. **2008**. Short-term influences on suspended particulate matter distribution in the northern Gulf of Mexico: satellite and model observations. *Sensors* 8:4249-4264.

D'Sa, E.J. and M. Korobkin. **2008a**. Examining SeaWiFS chlorophyll variability along the Louisiana coast using wavelet analysis. In: *Proceedings of the Oceans 2009 MTS/IEEE Conference. Biloxi, MS*. 5 p. IEEE Catalog Number: 0-933957-38-1.

D'Sa, E. J. and M. Korobkin. **2008b**. Colored dissolved organic matter in the northern Gulf of Mexico using ocean color: seasonal trends in 2005. In: *Proceedings of SPIE* 7105:710505.

D'Sa, E. J., and M. Korobkin. **2009**. Wind influence on chlorophyll variability along the Louisiana-Texas coast from satellite wind and ocean color data. In: *Proceedings of SPIE* 7473:747305.

D'Sa, E.J. and R.L. Miller. **2003**. Bio-optical properties in waters influenced by the Mississippi River during low flow conditions. *Remote Sensing of Environment* 84:538-549.

D'Sa, E.J., R.L. Miller, and C. Del Castillo. **2006**. Bio-optical properties and ocean color algorithms for coastal waters influenced by the Mississippi River during a cold front. *Applied Optics* 45:7410-7428.

D'Sa, E.J., R.L. Miller, and B.A. McKee. **2007**. Suspended particulate matter dynamics in coastal waters from ocean color: Application to the northern Gulf of Mexico. *Geophysical Research Letters* 34:L123611.

D'Sa, E. J., M. Korobkin, and D.S. Ko. **2011a**. Effects of Hurricane Ike on the Louisiana-Texas coast from satellite and model data. *Remote Sensing Letters* 2:1-11.

D'Sa, E.J., H. Roberts, and M.N. Allahdadi. **2011b**. Suspended particulate matter dynamics along the Louisiana-Texas coast from satellite observations. In: *Proceedings Coastal Sediments 2011*, p. 2390-2402.

Green, R.E. and R.W. Gould Jr. **2008**. A predictive model for satellite-derived phytoplankton absorption over the Louisiana shelf hypoxic zone: Effects of nutrients and physical forcing. *Journal of Geophysical Research* 113:C06005.

Green, R.E., R.W. Gould Jr. and D.S. Ko. **2008**. Statistical models for sediment/detritus and dissolved absorption coefficients in coastal waters of the northern Gulf of Mexico. *Continental Shelf Research* 28:1273-1285.

Henson, S.A. and A.C. Thomas. **2007**. Phytoplankton scales of variability in the California Current System: 1. Interannual and cross-shelf variability. *Journal of Geophysical Research* 112:C07017, 529-551.

Lohrenz, S.E., G.L. Fahnenstiel, D.G. Redalje, G.A. Lang, X. Chen, and M.J. Dagg. **1997**. Variations in primary production of northern Gulf of Mexico continental shelf waters linked to nutrient inputs from the Mississippi River. *Marine Ecology Progress Series* 1555:45-54.

Lohrenz, S.E., G.L. Fahnenstiel, D.G. Redalje, G.A. Lang, M.J. Dagg, T.E. Whitledge, Q. Dortch. **1999**. Nutrients, irradiance, and mixing as factors regulating primary production in coastal waters impacted by the Mississippi River plume. *Continental Shelf Research* 19:1113-1141.

Lohrenz, S.E., D.G. Redalje, W.-J. Cai, J. Acker, and M. Dagg. **2008**. A retrospective analysis and phytoplankton productivity in the Mississippi River plume. *Continental Shelf Research* 28:1466-1475.

Machu, E., B. Ferret, and V. Garcon. **1999**. Phytoplankton pigment distribution from SeaWiFS data in the subtropical convergence zone south of Africa: A wavelet analysis. *Geophysical Research Letters* 26:1469-1472.

Mannino, A., M.E. Russ, and S.B. Hooker. **2008**. Algorithm development and validation for satellite-derived distributions of DOC and CDOM in the U.S. Middle Atlantic Bight. *Journal of Geophysical Research* 113:C07051.

Morlet, J. **1983**. Sampling theory and wave propagation, In: C. H. Chen, ed. *Issues on acoustic signal/image processing and recognition. Vol. 1*. NATO ASI Series, Springer, Berlin. p. 233-261.

Naik, P., E.J. D'Sa, M. Grippo, R. Condrey, and J. Fleeger. **2011**. Absorption properties of shoal-dominated waters in the Atchafalaya Shelf, Louisiana, USA. *International Journal of Remote Sensing* 32:4383-4406.

O'Reilly, J.E., S. Maritorena, B.G. Mitchell, D.A. Siegel, K.L. Carder, S.A. Garver, M. Kahru, and C. McClain. **1998**. Ocean color algorithms for SeaWiFS. *Journal of Geophysical Research* 103:24937-24953.

Rabalais, N.N., R.E. Turner, Q. Dortch, D. Justic, V.J. Bierman, and W.J. Wiseman. **2002**. Nutrient-Enhanced productivity in the northern Gulf of Mexico: past, present and future. *Hydrobiologia* 47:39-63.

Sharma, N. and E.J. D'Sa. **2008**. Assessment and analysis of QuikSCAT vector wind products for the Gulf of Mexico: A long-term and hurricane analysis. *Sensors* 8:1927-1949.

Singh, S., E.J. D'Sa, and E. Swenson. **2010a**. Chromophoric dissolved organic matter (CDOM) variability in Barataria Basin using excitation-emission matrix (EEM) fluorescence and parallel factor analysis (PARAFAC). *Science of Total Environment* 408:3211-3222.

Singh, S., E.J. D'Sa, and E. Swenson. **2010b**. Seasonal variability in CDOM absorption and fluorescence properties in the Barataria Basin, Louisiana, USA. *Journal of Environmental Sciences* 22:1481-1490.

Torrence, C. and G.P. Compo, **1998**. A practical guide to wavelet analysis. *Bulletin American Meteorological Society* 79:61-78.

Vodacek, A., N.V. Blough, M.D. DeGrandpre, E.T. Pelzer, and R.K. Nelson. **1997**. Seasonal variation of CDOM and DOC in the Middle Atlantic Bight: Terrestrial inputs and photooxidation. *Limnology and Oceanography* 42:674-686.

Walker, N.D. and N.C. Rabalais. **2006**. Relationships among satellite chlorophyll a, river inputs, and hypoxia on the Louisiana continental shelf, Gulf of Mexico. *Estuaries and Coasts* 29:1081-1093.

Walker, N.D., R.R. Leben, and S. Balasubramanian. **2005**. Hurricane-forced upwelling and chlorophyll a enhancement within cold-core cyclones in the Gulf of Mexico. *Geophysical Research Letters* 32:L18610.

APPENDIX A

A peer reviewed, open-source article on CDOM absorption properties along the Louisiana coast was published with support from this funded study. This paper is included in its entirety beginning on the next page.

Citation: D'Sa, E.J., and S.F. DiMarco. **2009**. Seasonal variability and controls on chromophoric dissolved organic matter in a large river-dominated coastal margin. *Limnology and Oceanography,* 54(6), pp. 2233–2242.

The spring to summer seasonal transition in the spatial and vertical distribution of chromophoric dissolved organic matter (CDOM) optical properties were examined during surveys conducted in March, May, July, and August of 2005 in the waters influenced by the Mississippi-Atchafalaya River system of the NGOM. Strong seasonal river influences and a well-correlated inverse relationship between CDOM absorption at 412 nm and salinity during spring of 2005 suggest conservative mixing in the water column between the riverine freshwater sources and the oceanic end members. Trends in the CDOM absorption and the spectral absorption slope (*S*) and deviations from the end member conservative mixing line in surface and bottom waters during the summer suggest apparent sources and sinks of CDOM. Elevated CDOM in lower salinity surface waters at many stations appear linked to high dissolved oxygen (DO) concentrations (> 10 mg L^{-1}) and elevated chlorophyll concentrations. Effects of photooxidation in surface waters were observed as increasing *S* and enhanced CDOM loss in the ~27-32 salinity range and attributed to seasonal stratification and the increased solar radiation during the summer. In the bottom waters, elevated CDOM in the ~32-36 salinity range were associated with low DO and relatively higher bacterial abundance; this suggests a potential CDOM source due to microbial remineralization of organic matter in the bottom hypoxic zone. Seasonal dynamics associated with CDOM loss in surface waters and gains in bottom waters may be another pathway influencing hypoxia in coastal waters.

Limnol. Oceanogr., 54(6), 2009, 2233 2242
© 2009, by the American Society of Limnology and Oceanography, Inc.

Seasonal variability and controls on chromophoric dissolved organic matter in a large river-dominated coastal margin

Eurico J. D'Sa[a,*] and Steven F. DiMarco[b]

[a]Department of Oceanography and Coastal Sciences, Coastal Studies Institute, Louisiana State University, Baton Rouge, Louisiana
[b]Department of Oceanography, Texas A&M University, College Station, Texas

Abstract

The spring-to-summer seasonal transition in the spatial and vertical distribution of chromophoric dissolved organic matter (CDOM) optical properties was examined during surveys conducted in March, May, July, and August of 2005 in the waters influenced by the Mississippi–Atchafalaya River system of the northwestern Gulf of Mexico. Strong seasonal river influences and a well-correlated inverse relationship between CDOM absorption at 412 nm and salinity during spring of 2005 suggests conservative mixing in the water column between the riverine freshwater sources and the oceanic end members. Trends in the CDOM absorption and the spectral absorption slope (S) and deviations from the end-member conservative mixing line in surface and bottom waters during the summer suggest apparent sources and sinks of CDOM. Elevated CDOM in lower-salinity surface waters at many stations appears to be linked to high concentrations of dissolved oxygen (DO; >10 mg L^{-1}) and elevated chlorophyll concentrations. Effects of photo-oxidation in surface waters were observed as increasing S and enhanced CDOM loss in the ~27–32 salinity range and were attributed to seasonal stratification and the increased solar radiation during the summer. In the bottom waters, elevated CDOM levels in the ~32–36 salinity range were associated with low DO and relatively higher bacterial abundance; this suggests a potential CDOM source due to microbial remineralization of organic matter in the hypoxic zone in bottom waters. Seasonal dynamics associated with CDOM loss in surface waters and CDOM gains in bottom waters may be another pathway influencing hypoxia in coastal waters.

An important energy source in the microbial food web, dissolved organic matter (DOM) comprises a large fraction of organic molecules in the aquatic system (Hedges 1992). The optically active fraction of dissolved organic matter (chromophoric DOM or CDOM) forms a significant constituent of the DOM pool in natural waters and is derived allochthonously from terrestrial environments or autochthonously from in situ phytoplankton primary production or its microbial decomposition (Twardowski and Donaghay 2001; Rochelle-Newall and Fisher 2002). Microbial production of CDOM is associated with bacterial action on phytoplankton, natural dissolved organic carbon, zooplankton excretia, or algal exudates (Rochelle-Newall and Fisher 2002; Nelson et al. 2004). CDOM exhibits a featureless absorption spectrum that decreases exponentially with increasing wavelength from ultraviolet (UV) into visible wavelength, thus influencing the spectral distribution and light availability in the water column. The CDOM spectral slope (S) indicates the rate at which the CDOM absorption coefficient decreases with increasing wavelength. Changes in the shape of CDOM absorption spectrum or S have been attributed to solar photobleaching or photo-oxidation (increase in S) or to the differing natures of CDOM sources (Blough and Del Vecchio 2002; Twardowski and Donaghay 2002), thus providing additional insights into the nature of CDOM. Absorption of sunlight by CDOM has important implications to carbon cycling in the marine environment. For example, the process of photo-oxidation can result in photoproducts and a variety of organic compounds with low molecular weights (Zepp et al. 1998). Absorption by CDOM can mitigate the damaging effect of solar UV radiation in the aquatic system, while its loss due to photo-oxidation can decrease absorptivity in the UV and visible spectral regions. In the visible range of the electromagnetic spectrum, CDOM absorption can reduce the amount of photosynthetically active radiation (PAR) available to the phytoplankton and thus can affect primary productivity or can interfere with satellite determinations of seawater constituents such as phytoplankton pigments (Blough and Del Vecchio 2002).

Large CDOM optical signals are observed in coastal regions influenced by major rivers such as the Mississippi and the Orinoco, with CDOM generally decreasing with increasing salinity (Blough and Del Vecchio 2002). Seasonal variability in CDOM absorption and conservative mixing behavior with salinity have been reported in various coastal waters generally associated with terrestrial inputs from river discharge (Vodacek et al. 1997; D'Sa et al. 2003; 2006). The Mississippi–Atchafalaya system is the seventh largest river in the world in terms of freshwater and sediment flux, and it drains 41% of the continental United States. In addition to creating a major region of freshwater influence along the eastern Texas–Louisiana shelf (Nowlin et al. 2005), the river also transports large fluxes of organic and inorganic matter that strongly influence biogeochemical properties in the northern Gulf of Mexico (Dagg et al. 2004, 2007; Turner et al. 2007). Nutrient loading from the Mississippi and Atchafalaya Rivers stimulates high primary production that together with riverine particulate matter gives rise to intensified flux of particulate organic matter to the sea floor. Decomposition or remineralization of this

* Corresponding author: ejdsa@lsu.edu

organic matter via microbial respiration consumes oxygen which, together with vertical stratification due to increased warming of surface waters by solar radiation and reduced winds during the summer, have been linked to the formation of bottom hypoxia, a condition where dissolved oxygen (DO) concentrations in bottom waters are <2 mg L $^{-1}$ (equivalent to 63 μmol L $^{-1}$ or 1.4 mL L $^{-1}$; Wiseman et al. 1997; Rabalais et al. 2007; Hetland and DiMarco 2008).

The close coupling between dissolved organic carbon and CDOM observed in the coastal environment (Vodacek et al. 1997; Blough and Del Vecchio 2002) including the Mississippi River waters (Del Castillo and Miller 2008) suggest that CDOM could provide additional insights into biogeochemical processes and hypoxia occurring in the northern Gulf of Mexico. However, little is known about the relationship between the DO concentrations and CDOM absorption of the Louisiana–Texas coast. The complex physical, biological, and chemical processes in large river-dominated coastal margins have provided limited understanding on the sources (e.g., byproduct of primary production) and sinks (photo-oxidation) contributing to CDOM distribution and their optical properties (Chen et al. 2004; D'Sa 2008). In this study, an extensive suite of seasonal field measurements that include CDOM optical properties, salinity, DO concentrations and limited chlorophyll and bacterial abundance data were used to examine CDOM spatial and seasonal variation and the effects of photo-oxidation and remineralization of organic matter on CDOM optical properties and their linkages to low DO or hypoxic conditions in the study area.

Methods

The study site is located in the northern Gulf of Mexico on the Texas–Louisiana shelf (Fig. 1a) in waters largely influenced by the discharge from Mississippi–Atchafalaya river system, which delivers ~70% of the discharge through the Mississippi River's "bird's foot delta" into the deeper waters of the Gulf of Mexico. About 30% of the discharge is directed to the Atchafalaya River and into the Atchafalaya Bay and onto a broad, shallow shelf located ~250 km west of the bird's foot delta (Wiseman et al. 1997; Krug 2007). Coastal waters influenced by the Mississippi River from Southwest Pass to the Atchafalaya delta were sampled aboard the R/V *Gyre* during four cruises in the spring and summer of 2005 (Fig. 1a). During the March and May cruises, stations were occupied in regions A (west of Southwest Pass), B (off Terrebone Bay), and C (Atchafalaya shelf). In July, sampling was restricted to regions C and D due to the passage of Hurricane Dennis, which made landfall on 10 July in the eastern Gulf and followed Hurricane Cindy, which had passed through during the previous week. In August, regions B, C, and D (west of Atchafalaya shelf) were occupied as part of larger hypoxia study.

Water samples were generally collected from the surface, middle depths, and bottom depths in amber glass bottles with Teflon-lined caps (Niskin) during conductivity–temperature–depth (CTD) casts with a Sea-Bird Electronics CTD and a General Oceanics rosette system. The samples were then filtered through pre-rinsed 0.2-μm Nuclepore membrane filters within 3 h of collection. Spectral CDOM absorption [$a_{cdom}(\lambda)$] values of the filtered samples were obtained onboard the ship using a capillary wave-guide system (WPI, Inc.), a single-beam spectrophotometer (D'Sa et al. 1999, 2001) using a protocol described in Miller et al. 2002. The optical absorbance spectra A between 250 nm and 722 nm were determined from two scans: one of a cell filled with blank solution (Milli-Q) adjusted for the salinity of the sample, and one of the sample itself. The absorbance A was used as a baseline corrected by subtracting the absorbance at each wavelength from the average absorbance at the 715–722 nm band. The dimensionless absorbance spectra were converted to absorption coefficient (m $^{-1}$) at each wavelength λ, using the equation

$$a_{cdom}(\lambda) = 2.303(\lambda)/L \quad (1)$$

where L is the optical path length in meters (waveguide path lengths of 0.1 m or 0.5 m were used in the measurements). CDOM spectra typically fit a wavelength-dependent exponential function with a single slope parameter (S; nm $^{-1}$) such that $a_{cdom}(\lambda) = a_{cdom}(\lambda_0) \times e^{S(\lambda - \lambda_0)}$, where λ_0 was a reference wavelength. S was calculated using the linear least-squares regression of the logarithm of the CDOM spectral absorption between 370 nm and 550 nm.

Discrete DO concentrations were determined using the Winkler titration method and a SBE-43 DO probe (Sea-Bird). A fluorometer attached to the CTD rosette system provided fluorescence profiles that were converted to chlorophyll using chlorophyll estimates determined from discrete water samples using a calibrated fluorometer (Turner Designs). Bacterial abundances were determined after preparing and storing slides onboard at -20°C and then counting cells using epifluorescence microscopy on an Axioplan Imaging 2 universal microscope (Zeiss; Anitsakis 2006). River discharge data (Fig. 1b) were obtained from the U.S. Army Corps of Engineers monitoring stations located at Tarbert Landing, Mississippi, for the Mississippi River and at Simmesport, Louisiana, for the Atchafalaya River.

Results

Physical influences and CDOM optical properties—Although usual discharge from the Mississippi and Atchafalaya rivers peak in April–May (Fig. 1b), discharge was atypical in 2005; peak flow occurred in January, followed by a decreasing discharge for the remainder of the year (Fig. 1b). The March and May sampling periods followed the unusually early peak river discharge and the annual cycle of cold-air outbreaks that occur with characteristic time scales of 3 d to 10 d over the region during winter and spring, which results in cooling and mixing of the water column (Wiseman et al. 1997). Low levels of discharge from the Mississippi and Atchafalaya rivers characterized the cruises in July and August (Fig. 1b). Salinity of surface waters reflected the river discharge with lowest average

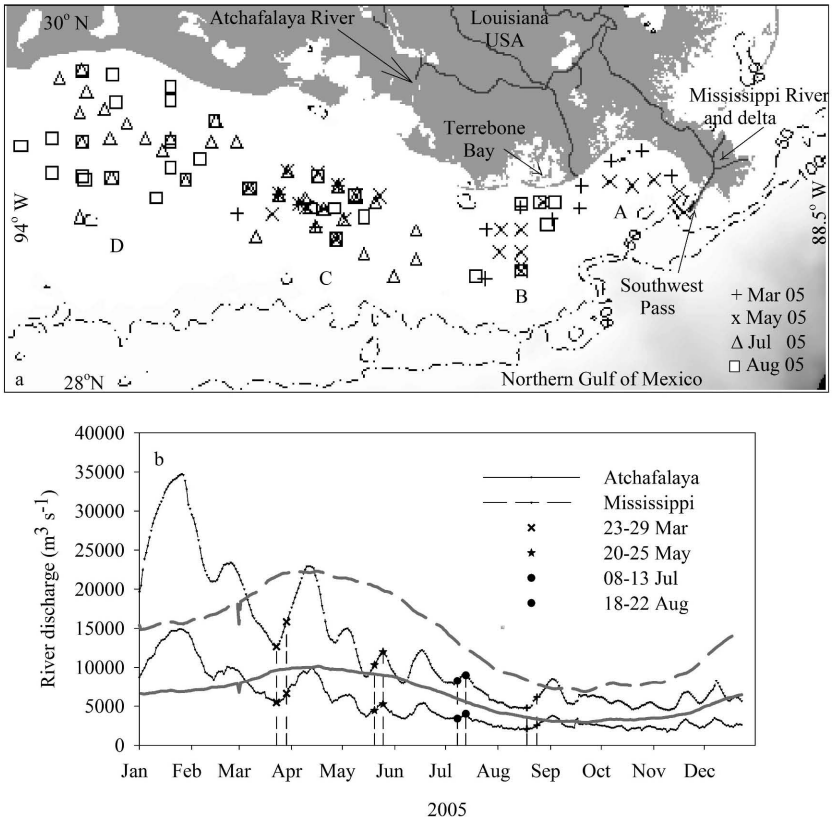


Fig. 1. (a) Study site in the northern Gulf of Mexico showing locations (regions A, B, C, and D) of CDOM sampling stations that were occupied during cruises in 23–29 March, 20–25 May, 08–13 July, and 18–22 August of 2005. (b) The Mississippi and Atchafalaya river discharge in 2005, with symbols indicating periods corresponding to four cruises. Dark gray lines indicate the mean discharge from the two rivers.

surface-water salinity in March (25.57 ± 1.64) that increased to 26.95 ± 0.46, 28.98 ± 0.31, and 28.48 ± 0.30, respectively during May, July, and August. Average salinity of bottom waters varied over a smaller range (34.68 ± 0.68, 34.51 ± 61, 31.98 ± 0.41, and 34.02 ± 0.36) during the same period. An anomalous increase in surface salinity (compared to August salinity) and a drop in bottom salinity in July 2005 could be attributed to the passage of Hurricane Cindy that made landfall on 05 July near region A (Grande Isle, Barataria Bay). Winds of up to 110 km h^{-1} before the hurricane made landfall mixed the water column (decreased bottom salinity) and probably elevated surface salinity and disrupted DO distribution in the study area.

CDOM optical properties plotted as a function of salinity reveal an inverse linear relationship between CDOM absorption at 412 nm, $a_{cdom}(412)$, and salinity (y = 1.37 – 0.036x, $r^2 = 0.93$, $n = 51$), indicating conservative mixing between the low-salinity river end members and the high-salinity ocean end member during March and May (Fig. 2a). The dependence of $a_{cdom}(412)$ on salinity appears to be conservative for the sampling regions A, B, and C influenced by both the Atchafalaya and Mississippi rivers. A previous study in region A (Del Castillo and Miller 2008) also documented a conservative CDOM–salinity relationship with slightly elevated slope (y = 1.60 – 0.04x, $r^2 = 0.84$, $n = 223$), indicating similar trends in the relationship. Large salinity differences (~9) between the surface and bottom waters in March 2005 (Fig. 3a) were associated with large $a_{cdom}(412)$ differences (surface: 0.54 ± 0.21 m^{-1} and bottom: 0.17 ± 0.13 m^{-1}). Although the CDOM–salinity relationship during early summer (July) appeared similar to that in the spring (Fig. 2c), there was greater

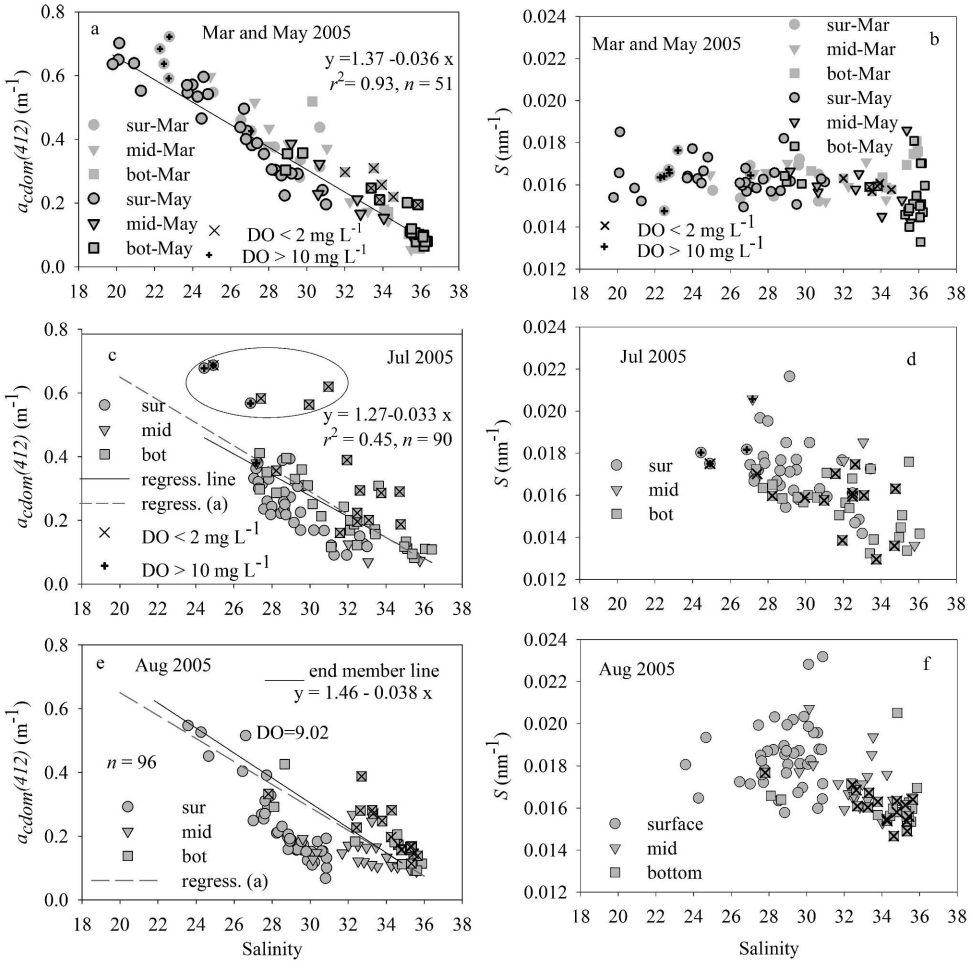


Fig. 2. CDOM absorption at 412 nm (m^{-1}) and the spectral slope (S; nm^{-1}) plotted as a function of salinity for samples (surface, middle depths, and bottom depths) obtained in (a, b) March and May, (c, d) July, and (e, f) August 2005. Solid lines denote the best-fit linear regression to the data for (a) and (c) and for the end-member line in (e) given by the relation y = 1.46 – 0.038x. Dashed lines in (c) and (e) denote the linear regression obtained in (a) and are shown for comparison.

scatter (r^2 = 0.45, n = 88) in the data with surface $a_{cdom}(412)$ in the ~27–32 salinity range lying below the conservative mixing line and a trend for higher values in their spectral slope (Figs. 2c,d, 3d). The $a_{cdom}(412)$ of bottom waters in the 32–35 salinity range, in contrast, tended to lie above the mixing line (Fig. 2c). With large deviations in CDOM between the surface and bottom waters in the mid-salinity range in August 2005 (Fig. 2e), low-salinity waters (<24) and high-salinity (>35) waters were used to define the end-member line (y = 1.46 – 0.038x; Rochelle-Newall and Fisher 2002; Yamashita and Tanoue 2004). This end-member line was similar to the spring CDOM–salinity conservative mixing line (Fig. 2a), suggesting insignificant seasonal changes in the end-member optical properties of CDOM during spring and summer of 2005.

The average S values of surface and bottom waters during March were 0.0160 ± 0.0002 and 0.0170 ± 0.0003 nm^{-1}, respectively (Figs. 2b, 3d). The lower S in surface waters reflects the terrestrial influences associated with high river discharge. The higher S in the higher-salinity bottom waters probably reflects oceanic influences

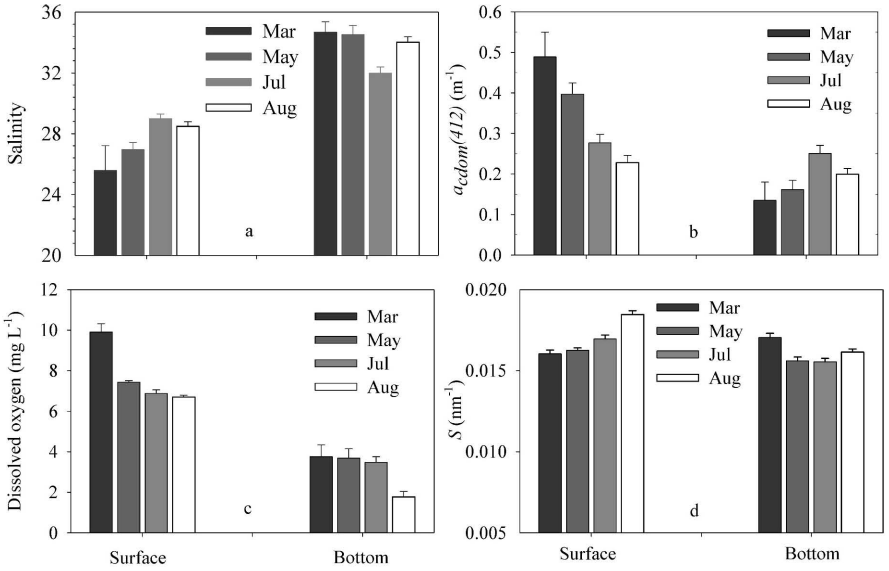


Fig. 3. Variation during March, May, July, and August 2005 for surface and bottom waters of (a) salinity, (b) $a_{cdom}(412)$, (c) dissolved oxygen (DO), and (d) spectral slope (S) for regions B, C, and D shown in Fig. 1. The error bars represent the SE of the mean.

and their compounded exposure to sunlight (Twardowski and Donaghay 2002). Average S gradually increased in surface waters to its highest value of 0.0185 ± 0.0002 nm^{-1} in August (Figs. 2d,f, 3d), indicating the increasing effects of photo-oxidation on CDOM. In contrast, a drop in the spectral slope of bottom waters to ~0.0156 ± 0.0002 nm^{-1} in May and July probably reflects contribution to CDOM from organic material fluxed to the bottom from the spring phytoplankton bloom. A slight increase in S to 0.0161 ± 0.0001 nm^{-1} in August (Figs. 2f, 3d) may be related to enhanced penetration of solar radiation in the summer (Lehrter et al. 2009). Some scatter in the absorption properties of bottom waters and surface waters could be due to the passage of Hurricane Cindy in July a few days prior to sampling, to the presence of different source waters (Chen and Gardner 2004), or to organic matter from the extensive coastal wetlands (Dagg et al. 2007). However, the conservative CDOM mixing in the shelf waters during spring cruises (March and May) followed by trends of increasing S values and deviation of the surface and bottom $a_{cdom}(412)$ values about the conservative end-member mixing line through the summer suggests potential seasonal loss and gain in CDOM in this river-dominated coastal margin.

CDOM absorption and dissolved oxygen—An examination of $a_{cdom}(412)$–salinity relationship (Fig. 2) and trends during March, May, July, and August 2005 in the salinity, DO concentrations, and CDOM optical properties [$a_{cdom}(412)$; S; Fig. 3] reveal different linkages between DO concentrations and CDOM of surface and bottom waters that deviated from the conservative end-member mixing line. In surface waters, elevated CDOM absorption was associated with higher levels of DO and phytoplankton biomass; in bottom waters, relatively high CDOM levels were associated with locations of low concentration of DO or hypoxia; a DO concentration of 2.0 mg L^{-1} is the accepted cutoff for hypoxia where most marine life is adversely affected.

During the March cruise, average DO concentration in surface waters was >9 mg L^{-1} (Fig. 3c) and was associated with higher chlorophyll fluorescence levels (not shown) compared with those measured in the summer cruises. At some stations with DO >10 mg L^{-1}, CDOM absorption deviated considerably from the conservative mixing line, indicating excess CDOM (Fig. 2a,c; circles marked with + sign). DO concentrations in surface waters decreased on average to 7.43 ± 0.66, 6.88 ± 1.07, and 6.70 ± 0.53 mg L^{-1}, respectively, in May, July, and August, and they were similarly accompanied by a decline in surface chlorophyll fluorescence observed during CTD casts (not shown). However, during the July cruise, at a few stations with supersaturated DO concentrations of ~12 mg L^{-1} (Fig. 2c; enclosed ellipse), large deviations from the conservative mixing line were associated with an elevated chlorophyll band observed in satellite imagery (D'Sa 2008). Similarly, during August, elevated surface CDOM was present at only one station with DO of 9.02 mg L^{-1} (Fig. 2e). Average S at stations with elevated DO concentrations were higher during March (0.0165 ± 0.0007 nm^{-1}, n = 9) and July (0.0186 ± 0.0013 nm^{-1}, n = 4) than the overall mean slopes for the two cruises.

Table 1. Salinity, oxygen, CDOM absorption at 412 nm $a_{cdom}(412)$, bacterial abundance (10^6 cells mL^{-1}), and chlorophyll concentrations measured at selected stations (regions A, B, and C) during March and May (shown as month 3 and month 5, respectively) for coincident data available for surface (~1.5 m) and bottom depths.

Station (month)	Site depth (m)	Salinity	Oxygen (mg L^{-1})	$a_{cdom}(412)$ (m^{-1})	Bacteria cells ($\times 10^6$ mL^{-1})	[Chl] (mg m^{-3})
		Sur (Bot)				
7A (3)	11.0	22.49(34.55)	10.53(1.57)	0.636(0.218)	3.0(5.0)	1.79(0.44)
11A (5)	11.9	20.14(35.70)	8.52(1.28)	0.702(0.347)	2.3(2.9)	2.32(0.32)
11B (5)	12.3	28.84(35.28)	6.21(0.74)	0.223(0.201)	5.1(3.6)	2.39(0.45)
7C (5)	10.3	26.87(28.98)	7.61(3.81)	0.425(0.354)	4.5(3.2)	2.76(0.38)
8C (5)	21.8	30.83(35.45)	6.81(5.73)	0.240(0.111)	1.5(2.2)	0.17(0.49)

Bacterial abundance during the study period ranged from 2.06×10^5 to 7.0×10^6 cells mL^{-1}, with a mean abundance of 1.72×10^6 cells mL^{-1} (Anitsakis 2006). Higher bacterial abundances were measured in the summer and closer to the shore and near the Mississippi River (zone A; Fig. 1a). Overall, correlations among bacterial abundance and DO concentration and salinity were negative, and they were positive with chlorophyll (Anitsakis 2006). Coincident measurements of bacterial abundance, CDOM, DO, and chlorophyll during spring (Table 1) and summer (Table 2) indicate bacterial abundance above the mean at stations with higher chlorophyll concentrations; however, direct microbial influences on CDOM of surface waters is not apparent due to higher CDOM in lower salinity waters and the masking effects of photo-oxidation in the summer.

Average trends in DO concentrations in bottom waters in regions B, C, and D revealed similar levels of DO during March and May (3.68 ± 1.84 mg L^{-1}), and they revealed a slightly lower level in July (3.47 ± 1.84 mg L^{-1}; Fig. 3c). During August, average DO levels decreased to 1.77 ± 1.46 mg L^{-1} (hypoxic waters). However, during March and May cruises, immediately west of the Mississippi delta (Fig. 1a, regions A and B), DO concentrations in bottom waters (at eight stations) were found to be hypoxic (Fig. 2a; squares marked with "×"). During the March and May cruises bottom waters at hypoxic stations indicated slightly elevated CDOM levels from the CDOM–salinity mixing line (Fig. 2a). High bacterial abundances were observed at these stations (Table 1), suggesting microbial degradation of organic matter. Elevated CDOM levels in bottom hypoxic waters were also observed during the July cruise (Fig. 2c) that appeared to be further enhanced at a few stations (Fig. 2c, enclosed ellipse) with very low DO (<0.5 mg L^{-1}) and associated with a band of high surface-chlorophyll concentrations observed in satellite imagery (D'Sa 2008). During the August cruise almost all the hypoxic stations in the ~32–36 salinity range showed excess CDOM (Fig. 2e). At many of these stations, in spite of the large differences between the low salinity in surface waters and high salinity in bottom waters, CDOM absorption differences were minimal or often higher in the bottom waters with low or hypoxic waters. Elevated levels of CDOM at these stations where measurements were available were often associated with higher concentrations of chlorophyll and elevated bacterial abundances (Table 2; stations 10D, 7C). Heterotrophic respiration associated with elevated organic matter could account for the low or hypoxic conditions in these bottom waters. Although, the spectral slope (S) of bottom waters at the hypoxic stations did not indicate seasonal trends, their values were lower than those of the surface waters suggesting different processes influencing CDOM distribution in the surface and bottom waters (Figs. 2b,d,f, 3d).

Surface CDOM sinks—CDOM absorption levels of a few surface samples in the ~27–32 salinity range during May cruise were below the conservative mixing line (Fig. 2a). This trend is more pronounced in July (Fig. 2c).

Table 2. Salinity, oxygen, CDOM absorption at 412 nm $a_{cdom}(412)$, bacterial abundance (10^6 cells mL^{-1}), and chlorophyll concentrations measured at selected stations (regions B, C, and D) during July and August (shown as month 7 and month 8, respectively) for coincident data available for surface (~1.5 m) and bottom depths.

Station (month)	Site depth (m)	Salinity	Oxygen (mg L^{-1})	$a_{cdom}(412)$ (m^{-1})	Bacteria cells ($\times 10^6$ mL^{-1})	[Chl] (mg m^{-3})
		Sur (Bot)				
7C (7)	11.2	27.43(28.76)	7.11(4.76)	0.418(0.394)	1.8(1.9)	0.49(2.18)
8C (7)	19.4	28.96(34.59)	7.57(2.58)	0.272(0.111)	2.3(2.1)	0.63(0.88)
17D (7)	20.0	31.12(33.61)	6.49(3.50)	0.121(0.308)	1.2(1.1)	0.09(0.54)
16D (7)	15.2	27.58(30.59)	6.48(4.51)	0.235(0.212)	0.2(1.1)	0.24(0.73)
11D (8)	12.7	24.26(34.36)	6.72(0.65)	0.525(0.197)	3.1(7.0)	1.0(0.30)
10D (8)	31.6	30.81(35.87)	6.31(2.86)	0.067(0.114)	2.1(2.3)	0.10(0.70)
7C (8)	10.4	27.93(32.44)	6.58(1.34)	0.327(0.227)	2.0(3.3)	0.75(0.99)
17D (8)	20.1	30.23(34.82)	6.68(4.98)	0.118(0.147)	2.1(1.7)	0.25(0.71)
16D (8)	15.5	28.31(33.78)	6.57(0.59)	0.212(0.248)	—(—)	0.39(0.13)

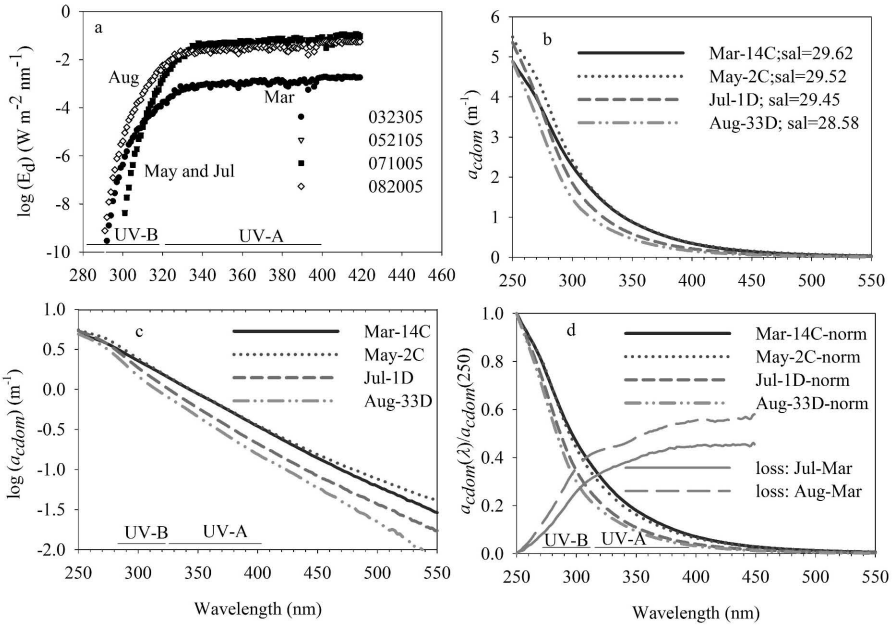


Fig. 4. (a) Noontime spectral down-welling irradiance E_d (W m^{-2} nm^{-1}) obtained from the TUV model (National Center for Atmospheric Research (NCAR), Colorado, USA) for a location off the Atchafalaya bay during 23 March, 21 May, 07 July, and 20 August 2005, (b) CDOM spectral absorption for surface samples at stations 14C, 2C, 1D, and 33D located in regions C and D (Fig. 1) during March, May, July, and August 2005, (c) log-linearized absorption spectra for stations in (b), and (d) comparison of fractional differences in (a) normalized at 250 nm and fractional loss for representative stations during July–March and August–March 2005.

It is most pronounced in August (Fig. 2e), indicating increasingly larger deficits in CDOM in the 27–32 salinity range as the sampling proceeded from spring into late summer. The conservative mixing of CDOM absorption in the surface waters (salinity <27) suggests a riverine signature that masks photobleaching effects. The exposure of these waters to solar radiation was insufficient to cause noticeable photobleaching. The average salinity of surface waters increased from March into May and July, which indicates the decreasing river discharge onto the shelf (Fig. 1b) followed by a slight decrease in August (Fig. 3a). As expected, the average surface CDOM absorption decreased from March to May to July to August (Fig. 3b). A decrease in salinity in August was expected to increase CDOM absorption; however, the large deficit in CDOM absorption observed in August in the 27–32 salinity range showed that the average CDOM absorption level was lower than that found in July. S in the ~27–32 salinity range of surface waters increased during the four cruises. Average S of the surface waters was the lowest in March (0.0160 ± 0.0008 nm^{-1}), increased gradually in May and July (0.0170 ± 0.0014 nm^{-1}), and showed the largest increase in August (0.0185 ± 0.0015 nm^{-1}; Fig. 3d), indicating the increasing effects of photo-oxidation on surface waters.

As the season progressed, the effects of reduced winds (Sharma and D'Sa 2008) and generally stronger summer stratification coupled with increase in solar radiation in both the UV wavelength (Fig. 4a) and the visible wavelength (Lehrter et al. 2009) appear to be the most likely factors leading to the amplification of the photo-oxidation effects during late summer. The variable deviations of surface $a_{cdom}(412)$ from the mixing line, the middle depth (between 5 and 10 m) $a_{cdom}(412)$ generally lying between the surface and the mixing line, and the increasing S (Fig. 2) suggest variable effects of photobleaching on the water samples that were probably dependent on the depth of solar penetration and the surface mixed layer. Thus, while the available data do not permit a quantitative assessment of the magnitude of losses due to photobleaching, a comparison of downward irradiance TUV model outputs (Troposphere Ultraviolet and Visible radiation model, National Center for Atmospheric Research, Colorado) in the 320–420 nm wavelength range (Fig. 4a) by month indicates an approximate two-order increase in irradiance in UV-A (320–400 nm) during May, July, and August 2005 when compared with March irradiance. A further increase into the UV-B waveband (280–320 nm) during August, a waveband that has been indicated to be most effective in DOM photolysis (Zepp et al. 1998), may

have enhanced the CDOM loss and may have caused a steepening of S (Del Vecchio and Blough 2002) of the surface waters during August. Assuming conservative mixing and same-source waters during spring and summer cruises, a comparison of surface waters at stations with similar salinities where deficits were observed in the summer indicate the largest spectral differences in CDOM in the UV (Fig. 4b). Spectral differences increased with increasing wavelength in the UV-B and further in the UV-A as indicated by the steeper slopes of the log-linearized absorption spectra for the summer surface samples and by the absorption spectra normalized at 250 nm (Fig. 4c,d). With photo-oxidation decreasing monotonically with increasing wavelengths, the comparisons also indicate greater losses in magnitude at shorter wavelengths although proportionally the losses are observed larger at longer wavelengths due to less initial absorption (Twardowski and Donaghay 2002).

Discussion

Deviations from a conservative CDOM–salinity relationship have been attributed to photo-oxidation resulting in loss of CDOM absorption and an increase in the spectral absorption slope (Vodacek et al. 1997; Twardowski and Donaghay 2002), to excess CDOM absorption associated with in situ production by phytoplankton either directly or microbially mediated, or to bottom resuspension events (Boss et al. 2001; Twardowski and Donaghay 2001; Yamashita and Tanaoue 2004). In this study, spatial and temporal patterns of CDOM optical properties in waters influenced by the Mississippi–Atchafalaya river system indicate conservative mixing throughout the water column between the riverine freshwater sources and the oceanic end member in the spring of 2005. Changes in CDOM optical properties (absorption at 412 nm and S) observed with the onset of summer, such as the deviations of surface waters and bottom waters from the conservative mixing line that intensified into late summer (August 2005), indicated seasonal changes of CDOM optical properties related to sources and sinks of CDOM in surface and bottom waters. Differences in the spectral slopes between surface waters and bottom waters indicate different processes influencing their optical properties.

Surface chlorophyll concentrations and DO levels were higher during the spring than in summer (Anitsakis 2006; Tables 1, 2). Surface $a_{cdom}(412)$ deviations from the CDOM–salinity mixing curve observed at stations in March, July, and August were generally found at stations with higher DO concentrations. In July at an algal bloom station with surface DO concentrations of 12.33 mg L^{-1}, highly elevated CDOM absorption (~45% excess) suggests a direct link between algal biomass and CDOM production. Although direct CDOM production by phytoplankton has not been observed (Rochelle-Newall and Fisher 2002), these observations strongly suggest rapid in situ biological production of CDOM either directly or microbially mediated (Twardowski and Donaghay 2001; Chen and Gardner 2004; Yamashita and Tanoue 2004). A previous study in the northern Gulf of Mexico documented coincident subsurface CDOM maxima and chlorophyll fluorescence that also provided evidence of in situ biological production of CDOM (Chen and Gardner 2004). Elevated bacterial abundance at stations with higher chlorophyll concentrations are consistent with previous observations of heterotrophic bacteria quickly responding to production of labile substrates with higher bacterial growth and abundance coinciding with increased primary production (Amon and Benner 1998). These stations with excess CDOM also exhibited slightly elevated spectral slopes consistent with previous measurements of in situ produced CDOM having higher values of S (Nelson et al 1998).

During the summer, surface waters exhibited a significant deficit in CDOM absorption (~42%) in the 27–32 salinity range and an increase in S, providing evidence of CDOM loss due to photo-oxidation and the alteration of the mainly terrestrially derived CDOM. While traces of photobleaching effects were detected in a previous study in the region (Chen and Gardner 2004; Conmy et al. 2004), similar seasonal effects on seawater CDOM were observed in the Middle Atlantic Bight (Vodacek et al. 1997). Previous observations of Mississippi River water exposed to sunlight indicated a substantial loss in riverine DOM, a decrease in its molecular size, and a decrease in reactivity due to photo-oxidation (Opsahl and Benner 1998). The high correlation between the DOC and CDOM (Del Castillo and Miller 2008) in coastal Louisiana waters further suggest similar transformations of CDOM in surface waters due to photo-oxidation. The deficit in CDOM absorption and the increase in slopes observed in July and August water samples in the middle salinity range in comparison with March samples suggest that the enhanced photo-oxidation could be attributed to the summer stratification and the cumulative exposure of these waters to increased solar radiation (Fig. 4a). Measurements of solar radiation during the summer (including 2005) across the Louisiana shelf indicated the euphotic depth (1% light level) almost always exceeded the surface mixed-layer depth and commonly intersected the bottom (Lehrter et al. 2009), suggesting CDOM in middle depths and some bottom waters could potentially undergo some photobleaching as indicated by elevated S in middle depths and bottom waters (Figs. 2d,f, 4d). The enhanced light and photochemical transformation of CDOM and DOM could also release organically bound nutrients that could stimulate phytoplankton production or result in more labile organic matter thus leading to enhanced microbial activity (Miller and Moran 1997; Bushaw-Newton and Moran 1999; Dagg et al. 2004).

Surface chlorophyll concentrations along the Louisiana shelf were observed to be much higher during the spring than in the summer (Anitsakis 2006; Tables 1, 2), and this trend is consistent with previous studies that show elevated primary production in the Mississippi River plume waters associated with seasonal river discharge. High levels of light absorption by both particulate and CDOM during spring (D'Sa et al. 2006) would generally limit light availability and thus primary productivity to the surface mixed layer. The flux of particulate organic matter to the sea floor or in

the water column below the pycnocline, and the respiratory processes associated with this material, have been indicated to contribute to the hypoxic conditions observed seasonally along the Louisiana coast (Rabalais et al. 2001). During spring, low DO or hypoxic waters were observed west of the Mississippi delta, and they were consistent with previous studies that have been attributed to strong river influence and eutrophic conditions that result mainly in water-column respiration contributing to the hypoxia (Hetland and DiMarco 2008). Elevated bacterial abundance associated with low DO concentrations and elevated CDOM levels at these stations suggest rapid bacterial remineralization of the organic matter contributing to the CDOM (Nelson et al. 2004).

During the summer, surface chlorophyll concentrations were lower in surface waters than in bottom waters (Anitsakis 2006; Tables 1, 2), mainly due to surface waters being nutrient limited. Nutrient concentrations were, however, slightly elevated in bottom waters (not shown). Loss of surface and subsurface CDOM due to photo-oxidation combined with reduced phytoplankton production during the summer could be a factor in recently reported studies showing increased light level in bottom waters and associated subsurface chlorophyll maxima (Lehrter et al. 2009). Low or hypoxic conditions were also observed over a larger area of the Louisiana Shelf during the summer (regions B, C, D). Most of the hypoxic bottom waters were associated with elevated CDOM that also had elevated chlorophyll concentrations and bacterial abundance (Table 2). Such increased levels of algal cells and detritus in subsurface waters were observed that were associated with enhanced bacterial growth and respiration and rapidly diminishing DO concentrations with depth (Amon and Benner 1998). In this study, bacterial abundance was relatively high in hypoxic waters during summer, with one of the highest bacterial counts (7×10^6 cells mL $^{-1}$) observed at a station with the lowest DO concentrations (0.65 mg L $^{-1}$), supporting the view that microbial remineralization (respiration) of both phytoplankton and its detrital component may have contributed to hypoxia and to the excess CDOM (~45%) at stations associated with hypoxia. However, in comparison to spring hypoxia observed west of the Mississippi delta, the hypoxia over a larger region of the Louisiana shelf may have been additionally stimulated by a combination of subsurface organic matter produced during the summer due to enhanced light availability in bottom waters and bacterial remineralization of this organic matter. Thus seasonal CDOM dynamics and the associated loss and gain in surface waters and bottom waters could provide additional pathways to hypoxia formation in the region through increased heterotrophic activity associated with increased and more labile organic biomass (both particulate and dissolved). The nonconservative behavior of CDOM at some salinity ranges due to its photo-oxidation or production suggest that its use as a water mass or salinity tracer needs to be used with caution. A large and variable increase in S during the summer also suggests that semi-analytic ocean-color algorithms may need to account for seasonal changes in the spectral slope to obtain more accurate estimates of optical parameters from satellite data.

Acknowledgments

We thank the Captain and crew of the R/V *Gyre* and many graduate students who assisted with sampling. This work was funded by the Minerals Management Service (MMS) Cooperative Agreement M08AX12685 and by a National Aeronautics Space Administration (NASA) Decisions Support Grant NNA07CN12A (Applied Sciences Program) to D'Sa. Hypoxia cruises were funded by the National Oceanic and Atmospheric Administration (NOAA) N-GOMEX grants (NA03NOS4780039 and NA06NOS4790198) to Di Marco.

References

Amon, R. M. W., and R. Benner. 1998. Seasonal patterns of bacterial abundance and production in the Mississippi River plume and their importance for the fate of enhanced primary production. Microbial Ecol. **35:** 289–300.

Anitsakis, E. C. 2006. Dynamics of marine pelagic bacterial communities on the Texas-Louisiana shelf. M.S. thesis. Texas A&M University.

Blough, N. V., and R. Del Vecchio. 2002. Chromophoric dissolved organic matter (CDOM) in the coastal environment, p. 509–546. *In* D. Hansell and C. Carlson [eds.], Biogeochemistry of marine dissolved organic matter. Academic Press.

Boss, E., W. S. Pegau, Z. N. V. Zaneveld, and H. Barnard. 2001. Spatial and temporal variability of absorption by dissolved material at a continental shelf. J. Geophys. Res. **106:** 9499–9507.

Bushaw-Newton, K. L., and M. A. Moran. 1999. Photochemical formation of biologically available nitrogen from dissolved humic substances in coastal marine systems. Aquat. Microb. Ecol. **18:** 285–292.

Chen, R. F., and G. B. Gardner. 2004. High-resolution measurements of chromophoric dissolved organic matter in the Mississippi and Atchafalaya River plume regions. Mar. Chem. **89:** 103–125.

Conmy, R. N., P. G. Coble, R. F. Chen, and G. B. Gardner. 2004. Optical properties of colored dissolved organic matter in the Northern Gulf of Mexico. Mar. Chem. **89:** 127–144.

Dagg, M. J., J. W. Ammerman, R. M. W. Amon, W. S. Gardner, R. E. Green, and S. E. Lohrenz. 2007. A review of water column processes influencing hypoxia in the northern Gulf of Mexico. Estuaries and Coasts **30:** 735–752.

———, R. Benner, S. Lohrenz, and D. Lawrence. 2004. Transformation of dissolved and particulate materials on continental shelves influenced by large rivers: Plume processes. Cont. Shelf Res. **24:** 833–858.

Del Castillo, C. E., and R. L. Miller. 2008. On the use of ocean color remote sensing to measure the transport of dissolved organic carbon by the Mississippi River plume. Remote Sens. Environ. **112:** 836–844.

Del Vecchio, R., and N. V. Blough. 2002. Photobleaching of chromophoric dissolved organic matter in natural waters: Kinetics and modeling. Mar. Chem. **78:** 231–253.

D'Sa, E. J. 2008. Colored dissolved organic matter in coastal waters influenced by the Atchafalaya River, USA: Effects of an algal bloom. J. Appl. Remote Sens. **2:** 023502, doi: 10.1117/1.2838253.

———, and R. L. Miller. 2003. Bio-optical properties in waters influenced by the Mississippi River during low flow conditions. Remote Sens. Environ. **84:** 538–549.

———, ———, and C. Del Castillo. 2006. Bio-optical properties and ocean color algorithms for coastal waters influenced by the Mississippi River during a cold front. Appl. Opt. **45:** 7410–7428.

———, and R. G. Steward. 2001. Liquid capillary waveguide application in absorbance spectroscopy. Limnol. Oceanogr. **46:** 742–745.

———, ———, A. Vodacek, N. V. Blough, and D. Phinney. 1999. Optical absorption of seawater colored dissolved organic matter determined using a liquid capillary waveguide. Limnol. Oceanogr. **44:** 1142–1148.

Hedges, J. I. 1992. Global biogeochemical cycles: Progress and problems. Mar. Chem. **39:** 67–93.

Hetland, R. D., and S. F. DiMarco. 2008. How does the character of oxygen demand control the structure of hypoxia on the Texas-Louisiana continental shelf? J. Mar. Systems **70:** 49–62.

Krug, E. C. 2007. Coastal change and hypoxia in the northern Gulf of Mexico: Part I. Hydrol. Earth Syst. Sci. **11:** 180–190.

Lehrter, J. C., M. C. Murrell, and J. C. Kurtz. 2009. Interactions between freshwater input, light, and phytoplankton dynamics on the Louisiana continental shelf. Cont. Shelf. Res. **29:** 1861–1872.

Miller, R. L., M. Belz, C. E. Del Castillo, and R. Trzaska. 2002. Determining CDOM absorption spectra in diverse aquatic environments using a multiple pathlength, liquid core waveguide system. Cont. Shelf Res. **22:** 1301–1310.

Miller, W. L., and M. A. Moran. 1997. Interaction of photochemical and microbial processes in the degradation of refractory dissolved organic matter from a coastal marine environment. Limnol. Oceanogr. **42:** 1317–1324.

Nelson, N. B., C. A. Carlson, and D. K. Steinberg. 2004. Production of chromophoric dissolved organic matter by Sargasso Sea microbes. Mar. Chem. **89:** 273–287.

Nowlin, W. D., Jr., A. E. Jochens, S. F. DiMarco, R. O. Reid, and M. K. Howard. 2005. Low frequency circulation over the Texas-Louisiana shelf, p. 219–240. *In* W. Sturges and A. Lugo-Fernandez [eds.], Circulation of the Gulf of Mexico: Observations and models. AGU.

Opsahl, S., and R. Benner. 1998. Photochemical reactivity of dissolved lignin in river and ocean waters. Limnol. Oceanogr. **43:** 1297–1304.

Rabalais, N. N., R. E. Turner, and E. J. Wiseman, Jr. 2001. Hypoxia in the Gulf of Mexico. J. Environ. Qual. **30:** 320–329.

———, ———, B. K. Sen Gupta, D. F. Boesch, P. Chapman, and M. C. Murrell. 2007. Hypoxia in the Northern Gulf of Mexico: Does the science support the plan to reduce, mitigate, and control hypoxia? Estuaries and Coasts **30:** 753–772.

Rochelle-Newall, E. J., and T. R. Fisher. 2002. Production of chromophoric dissolved organic matter fluorescence in marine and estuarine environments: An investigation into the role of phytoplankton. Mar. Chem. **77:** 7–21.

Sharma, N., and E. J. D'Sa. 2008. Assessment and analysis of QuikSCAT vector wind products for the Gulf of Mexico: A long-term and hurricane analysis. Sensors **8:** 1927–1949.

Turner, R. E., N. N. Rabalais, R. B. Alexander, G. McIsaac, and R. W. Howarth. 2007. Characterization of nutrient, organic carbon, and sediment loads and concentrations from the Mississippi River into the northern Gulf of Mexico. Estuaries and Coasts **30:** 773–790.

Twardowski, M. S., and P. L. Donaghay. 2001. Separating in situ and terrigenous sources of absorption by dissolved materials in coastal waters. J. Geophys. Res. **106:** 2545–2560.

———, and ———. 2002. Photobleaching of aquatic dissolved materials: Absorption removal, spectral alteration, and their interrelationship. J. Geophys. Res. **107:** 3091, doi: 10.1029/1999JC000281.

Vodacek, A., N. V. Blough, M. D. DeGrandpre, E. T. Peltzer, and R. K. Nelson. 1997. Seasonal variation of CDOM and DOC in the Middle Atlantic Bight: Terrestrial inputs and photo-oxidation. Limnol. Oceanogr. **42:** 674–686.

Wiseman, W. J., Jr., N. N. Rabalais, R. E. Turner, S. P. Dinnel, and A. MacNaughton. 1997. Seasonal and interannual variability within the Louisiana coastal current: Stratification and hypoxia. J. Mar. Systems **12:** 237–248.

Yamashita, Y., and E. Tanoue. 2004. In situ production of chromophoric dissolved organic matter in coastal environments. Geophys. Res. Lett. **31:** L14302, doi: 10.1029/2004GL019734.

Zepp, R. G., T. V. Callaghan, and D. J. Erickson. 1998. Effects of enhanced solar ultraviolet radiation on biogeochemical cycles. J. Photochem. Photobio. B: Biol. **46:** 69–82.

Associate editor: Dariusz Stramski

Received: 02 April 2009
Accepted: 25 July 2009
Amended: 10 August 2009

The Department of the Interior Mission

As the Nation's principal conservation agency, the Department of the Interior has responsibility for most of our nationally owned public lands and natural resources. This includes fostering the sound use of our land and water resources; protecting our fish, wildlife, and biological diversity; preserving the environmental and cultural values of our national parks and historical places; and providing for the enjoyment of life through outdoor recreation. The Department assesses our energy and mineral resources and works to ensure that their development is in the best interests of all our people by encouraging stewardship and citizen participation in their care. The Department also has a major responsibility for American Indian reservation communities and for people who live in island communities.

The Bureau of Ocean Energy Management Mission

The Bureau of Ocean Energy Management (BOEM) promotes energy independence, environmental protection, and economic development through responsible, science-based management of offshore conventional and renewable energy.